Final Technical Report for US Department of Energy Project

Contract: DE-FG02-03ER63674

Multi-level kinetic and dynamic biologically based risk models for low dose radiation

Executive Summary

In this project we provide an example of how to develop multi-tiered models to go across levels of biological organization to provide a framework for relating results of studies of low doses of ionizing radiation. This framework allows us to better understand how to extrapolate laboratory results to policy decisions, and to identify future studies that will increase confidence in policy decisions.

Conceptual Model Framework

In this final report and the accompanying appendices we provide support for our central premise that to model the vast array of low dose radiation data available, a multi-dimensional modeling framework is required. The underlying construct for this framework is illustrated in Figure 1. In this framework we envision the need to 1) evaluate mechanistic data from multiple levels of biological organization, 2) evaluate data across species and 3) evaluate both individual and human population (epidemiological) data. The dimensions of dose and time frame these evaluations.

On the left axis of Figure 1, various levels of biological assessment are listed and this parallels the levels of biological organization. Moving across the x-axis, three concepts are illustrated: 1) cross-species extrapolation from rodents to humans, 2) *in vitro* to *in vivo* comparisons and 3) individual versus population level assessments.

The radiation literature is unique in that there are so many sources of data available that support low dose estimation of risks in humans. These data sets provide data for models to quantify how to go from *in vitro* to *in vivo* data, and extrapolate results for humans from rodents. To move across these levels of assessment or across populations, kinetic and dynamic models are needed to relate response across dose and time. Inherent in these multilevel assessments is the need for consideration of severity of effect. Relating significance or severity of effect at biochemical and molecular response levels and using distributional modeling approaches will allow for better linkage of the impacts at multiple levels of observation. These observations are similar to the biomarker paradigm where individual responses are evaluated as to the point where they move from a measurable effect to an early indication of an adverse impact, to clear evidence of an

adverse impact, and ultimately to disease. Such models can provide the context and framework where new scientific data can be added and the importance of the new data for risk estimates can be clearly determined.

In this project we showed how to develop models in the areas inside of the dotted boxes in Figure 1. In the future we will attempt to expand the regions of biological organization and assessment in Figure 1as experimental data becomes available to increase support of our premise that multilevel modeling provides a framework for understanding how to predict and understand adverse impacts of radiation in humans.

Application of Conceptual Framework to the Effects of Low Dose Ionizing Radiation on the Developing Brain

In our application of the Conceptual Model we were able to move across multiple levels of biological assessment for rodents going from molecular to organism level for in vitro and in vivo endpoints and to relate these to human in vivo organism level effects. We used the rich literature on the effects of ionizing radiation on the developing brain in our models.

Developing Brain: The developing brain is unique compared to other fetal organs for several reasons. The brain is especially complex in structure, with various regions and individual cells having specific identities and functions. Development of these regions is not synchronous, but takes place at specific intervals over various periods of time (*1*). Proper brain function is determined by the interconnection of various cells and structures. Normal structure depends on an orderly sequence of events, which must occur linearly in time and space *(2*). Lastly, central nervous system neurons cannot replicate, so alterations during development are often permanent and irreparable. Due to its unique and complex structure and dependence on the specific timing of events, the developing neocortex is acutely sensitive to toxicant exposure (*3*). A wide range of chemical exposures, environmental conditions, and nutritional factors can have permanent deleterious effects on the developing brain.

In order to understand the effects of radiation on the developing brain it was necessary to characterize normal development of the brain. An interspecies model was developed for this pupose (24,25) to simulate acquisition of neocortical neuronal number across mammalian species. Extrapolating from rodents to humans it was important to model the accelerated enlargement of the neocortex during human evolution. Neocortex development is marked by discrete stages of neural progenitor cell proliferation and death, neuronal differentiation, and neuronal programmed cell death. Computational models were based on experimentally derived parameters of cell cycle length, commitment to cell cycle exit, and cell death. Comparisons of primate models with previously developed rodent models suggest a lengthening of the duration of neuronogenesis and of the cellular processes of cell cycle progression and death can account

for the increase in size of the primate neocortex. Compared with rodents cell death may play a larger role in the developing primate neocortex. Our mathematical models of the development and evolution of the neocortex provide a biological basis for extrapolation between rodent and humans.

Radiation has been a thoroughly researched and well-documented neurological teratogen that can have significant effects on brain development (4). The most compelling effects were observed among the atomic bomb survivors. The most severely affected individuals were exposed between 8-15 weeks of gestation, a period of rapid replication of neuronal precursor cells and neuron differentiation (*5*). A clear dose- response relationship was observed in this population. Of those individuals exposed during this time to doses between 1-2 Gy, 62.5% were classified as mentally retarded and 29% were affected at a dose less than 1 Gy (*6*). Low-dose exposures can cause less obvious effects, such as reduced learning ability and subtle behavioral differences. In the late 1950s, IQ tests were administered to many atomic bomb survivors who were exposed *in utero* to doses less than 50 cGy (*7*). Data on school performance in elementary school grades one through four also were collected. These data suggest that radiation exposure, especially exposures that occurred 8 to 15 weeks after conception, had a negative impact on both outcomes. For survivors exposed to a low dose (around 20 cGy), the loss of IQ was estimated to be about 5 points.

Radiation Effects on Migration of Neurons in the Neocortex: The developed mammalian neocortex is composed of six thin layers of neurons, each identified by the neuron type and the pattern of interconnections. After completing their last mitosis in the ventricular zone (VZ), cortical neurons undergo a long migratory process through the intermediate zone (IZ, the future white matter) toward the cortical plate (CP, the future gray matter) (*8*). The complex pattern of neuron migration in the mammalian cerebral cortex has been termed ‘inside-out’. As cells exit the cell cycle, the earliest formed neurons travel a short distance and occupy the deepest cortical layer (layer VI). Later-formed neurons must migrate past those generated earlier to occupy progressively more superficial layers. Thus, neurons forming layer I are formed last and must travel farthest, past the other five layers (*9*). Upon reaching a final location within the cortical plate, neurons differentiate and form functional units.

The focus of this report is on disrupted neuronal migration due to radiation exposure and the structural and functional implications of these early biological effects. The cellular mechanisms resulting in pathogenesis are most likely due to a combination of the three mechanisms mentioned. For the purposes of a computational model, quantitative studies of low dose radiation effects on migration of neuronal progenitor cells in the cerebral mantle of experimental animals were used.

Death of Neurons Caused by Radiation in the Developing Neocortex: Radiation exposures that cause mental retardation, reduced learning ability and subtle behavioral differences we

hypothesize are also due to an aberrant loss of neuronal precursor cells or inappropriate cell death among post-mitotic neuronal cells in the developing brain, which can result in a decreased neuron number in the mature brain (11, 12, 13, 24, 25, 26, 27, 28, 29, 30, 32). Considering that a single precursor cell present at E11 (that is 11 days after gestation) in the mouse is estimated to contribute over 250 neurons to the final population (14), cell death of these early cells due to toxicant exposure can have a substantial impact on neuron production. Various toxicants have been shown to result in decreased neuron number through the induction of apoptosis in neuronal precursor cells or post-mitotic neurons following an exposure during neurogenesis, including radiation (15, 29, 30, 32), methylmercury (16), and ethanol (17).

Many studies have demonstrated that extensive cell death is induced in the developing murine cerebral cortex within a few hours after radiation exposure. Surviving fetuses typically have abnormal behavior patterns and deficits in neurological function (18, 30, 32). Therefore, it is hypothesized that neural cell death is a primary component in the radiation-induced abnormal development of the mammalian brain. This portion of the computational model that we developed aims at quantitatively determining how radiation-induced cell death of neuronal precursor cells affects the number of post-mitotic neurons at the end of the neurogenesis period.

Models of Radiation Effects on Neuron Migration and Death in the Neocortex

Neuron Migration Model Framework: The basic framework for this developmental model was adapted from the model of Leroux *et al*. (*19, 25*), which describes organogenesis through the processes of cellular replication, differentiation, and death (Figure 2). The model defines X cells as neuronal precursor cells. Each X cell can replicate and form two X daughter cells or differentiate into a post-mitotic neuron, Y cell. The model can be modified to accommodate replication events that produce one X cell and one Y cell. The X cell replication rate (λ) and the transformation rate (ν) are time dependent. Both X and Y cells undergo cell death at a specified background rate (μ). Replication and differentiation rates for X cells, corresponding to neuronal precursor cells in the fetal mouse, are incorporated from published literature. The division rate of Y cells is set to zero to simulate a terminally differentiated status.

To simplify the mechanism of neuronal migration, the framework for the migration model is summarized as follows: neuronal precursor cells (X cells) exit the cell cycle and become undifferentiated, migratory neurons (M cells). M cells then transform into differentiated neurons (Y cells) once they cease migration at a biologically determined location. The rate at which cells transition from M cells to Y cells is represented by ν_2. Various mechanistic data for the effects of radiation can be incorporated into this ν rate (see appendix).

According to the model, upon radiation exposure at the beginning of neurogenesis, the transformation of post-mitotic neuronal cells (M) into neurons (Y) is slowed. The decreased transition rate (ν_2) is due to a slower migration of M cells. In a dose-dependent manner, M cells

accumulate in the neocortex (Figure 3.A). Likewise, the number of Y cells does not peak until later in development (Figure 3 B). A 10 cGy exposure does not lead to major alterations in the growth of the Y cell population. At P5, the day when all M cells complete migration in control brains, the exposed brain has only 2.5% of its M cells still migrating. According to our predictions, these remaining 50,000 cells would complete migration within two days, or by P7. A 25 cGy exposure leads to a 75% decrease in the rate of transition between M cells and Y cells (v_2). This leads to a sustained presence of migrating cells, M, in the neocortex. Y cells may eventually reach control levels, but it would require an additional 25 days for this to occur (26, 27, 28, 29, 30, 32).

The incorporation of neuronal migration adds valuable information to our model of neurogenesis. This process is highly susceptible to toxicant exposure and alterations in migration have been associated with several pathological manifestations (*10,* 29, 30, 32). Through the incorporation of parameters describing neuronal migration, we can more accurately assess how toxicants affect neurodevelopment. The model can also be used to predict relative neuron position in addition to neuron number.

Overall, these studies do support the current predictions of our model, in which radiation exposure results in a disorganized neuronal cytoarchitecture in the postnatal neocortex. Postnatal neurodevelopment in the mouse includes synaptogenesis, and the presence of irregularly placed neurons can lead to failed connections or misconnections between neurons. We conclude that this abnormal cytoarchitecture within the developing neocortex is the basis for some of the neurobehavioral and intellectual deficits observed in animals and humans prenatally-exposed to ionizing radiation and other toxicants.

The basic neurogenesis model was expanded to incorporate changes in cell death rates caused by radiation exposure in utero. The model framework is shown in Figure 4, in which the dose-dependent parameter of clearance time, ct, is added to better describe radiation-induced cell death processes. All model rates in the unexposed murine neocortex were calculated from experimental data.

The bystander effect is the adverse response of unexposed cells when neighboring cells are irradiated (20, 28). Typically, this effect is more pronounced when the cells are grouped in high-density areas, where cell- cell contact and communication is high (21, 28). Because we expected that cells on E11 would have the highest rates of cell death (in relationship to the high rates of replication), this bystander phenomenon might explain why we observe higher sensitivity of cells in the E13 mouse to undergo cell death in the VZ. At this developmental time point, the VZ contains approximately 7 millions neuronal precursor cells, which is the peak density in this region across developmental time (Figure 5). In comparison, the proliferative region contains only 500,000 and 1 million cells on E11 and E15, respectively. Therefore, it is possible that E13 has the highest cell death rates due to the bystander effect.

There is a lack of comparable estimates of neuron production following *in utero* irradiation at low doses in rodent models, however comparison of the model output to behavioral endpoints can be informative. Table 1 displays the no observable adverse effect level (NOAEL) and the lowest observable adverse effect level (LOAEL) for behavioral effects in mice exposed to low doses of radiation during neurogenesis. Baskar & Uma Devi (*22*) determined that learning delays, assessed by the hole board test, were present in animals exposed to 35 cGy on E11.5 and E12.5. According to our model predictions, this corresponds to 10% of neuron improperly located within the neocortex on P5. Animals exposed on E14.5 did not demonstrate a learning delay until the exposure reached 50 cGy, related to a 5% reduction in neurons. Exposure on E17.5 did not affect learning behavior, and our model predicts very small decreases in neuron production after exposure at this time (24, 25, 26, 27, 28, 29, 30, 32). A second study by Hossain & Uma Devi (*23*) determined the NOAEL for memory retention was 25 cGy when exposure occurred on E14. Model predictions indicate that 5% of post-mitotic neurons would be improperly located on P5.

Currently, our model does not make any assumptions as to the exact mechanism of migration disruption following irradiation. More detailed information pertaining to migratory disruption, such as dose-response data for damage to radial glial fibers or changes in protein expression, can easily be incorporated into the model. This information would provide insight into toxicant-specific mechanisms and enable the use of more *in vitro* data in our developmental dose-response model (31). Future developments of this model include the addition of this detailed information into the model in order to gain a better understanding of normal neuron migration and how toxicant exposure alters this sensitive process (25, 32).

In this project we were able to show now results from studies of low doses of radiation can be used in a multidimensional framework to construct linked models of neurodevelopment using molecular, cellular, tissue, and organ level studies conducted both in vitro and in vivo in rodents. These models could also be linked to behavioral endpoints in rodents which can be compared to available results in humans. The available data supported modeling to 10 cGy with limited data available at 5 cGy. We observed gradual but non-linear changes as the doses decreased. For neurodevelopment it appears that the slope of the dose response decreases from 25 cGy to 10 cGy. Future studies of neurodevelopment should be able to better define the dose response in this range.

References

1. J. Berger-Sweeney and C. F. Hohmann. Behavioral consequences of abnormal cortical development: insights into developmental disabilities. *Behav Brain Re.* **86**, 121-42 (1997).
2. L.G. Costa, M. Aschner, A. Vitalone, T. Syversen, and O.P. Soldin**.** Developmental neuropathology of environmental agents. *Annu Rev Pharmacol Toxicol* **44,** 87-110 (2004).

3. P.M. Rodier. Environmental causes of central nervous system maldevelopment. *Pediatrics* **113,** 1076-83 (2004).
4. R.L. Brent. The effects of ionizing radiation, microwaves, and ultrasound on the developing embryo: clinical interpretations and applications of the data. *Curr Probl Pediatr*. 14, 1-87 (1984).
5. W.J. Schull and M. Otake. Cognitive function and prenatal exposure to ionizing radiation. *Teratology* **59,** 222-6 (1999).
6. W.J. Schull. Ionising radiation and the developing human brain. *Ann ICRP* **22,** 95-118 (1991).
7. M. Otake and W.J. Schull. A review of forty-five years study of Hiroshima and Nagasaki atomic bomb survivors. Brain damage among the prenatally exposed. *J Radiat Res* **32**, 249-64 (1991).
8. B. Nad arajah, P. Alifragis, R.O. Wong, and J.G. Parnavelas. Neuronal migration in the developing cerebral cortex: observations based on real-time imaging. *Cereb Cortex* **13**, 607-11 (2003).
9. M.P. Ignacio, E.J. Kimm, G.H. Kageyama, J. Yu, and R.T. Robertson. Postnatal migration of neurons and formation of laminae in rat cerebral cortex. *Anat Embryol* **191**, 89-100 (1995).
10. B.F. Uher and J. A. Golden. Neuronal migration defects of the cerebral cortex: a destination debacle. *Clin Genet* **58**, 16-24 (2000).
11. I. Ferrer, S. Alcantara, M.J. Zujar, and C. Cinos. Structure and pathogenesis of cortical nodules induced by prenatal X-irradiation in the rat. *Acta Neuropathol (Berl).* **85**, 205-12 (1993).
12. C.J. D'Amato and S.P. Hicks. Effects of low levels of ionizing radiation on the developing cerebral cortex of the rat. *Neurology*. **15**, 1104-16 (1965).
13. M. Berry and J.T. Eayrs. The effects of x-irradiation on the development of the cerebral cortex. *J Anat*. 100, 707-22 (1966).
14. V.S. Caviness, T. Takahashi, and R.S. Nowakowski. Numbers, time and neocortical neuronogenesis: a general developmental and evolutionary model. *Trends Neurosci* **18**, 379-83 (1995).
15. T. Miki, Y. Fukui, Y. Takeuchi, and M. Itoh. A quantitative study of the effects of prenatal X-irradiation on the development of cerebral cortex in rats. *Neurosci Res* **23**, 241-7 (1995).
16. A. Kakita, K. Wakabayashi, M. Su, Y. Yoneoka, M. Sakamoto, F. Ikuta, and H. Takahashi. Intrauterine methylmercury intoxication. Consequence of the inherent brain lesions and cognitive dysfunction in maturity. Brain Res **22**, 322-30 (2000).
17. M.W. Miller. Kinetics of the migration of neurons to rat somatosensory cortex. *Brain Res Dev Brain Res* **115**, 111-22 (1999).
18. E. Rola, J. Raber, A. Rizk, S. Otsuka, S.R. VandenBerg, D.R. Morhardt, and J.R. Fike. Radiation-induced impairment of hippocampal neurogenesis is associated with cognitive deficits in young mice. *Exp Neurol* **188**, 316-30 (2004).
19. B.G. Leroux, W.M. Leisenring, S.H. Moolgavkar, and E.M. Faustman. A biologically-based dose-response model for developmental toxicology. *Risk Anal* **16**, 449-58 (1996).
20. Brooks AL. Evidence for 'bystander effects' in vivo. *Hum Exp Toxicol*. **23**, 67-70 (2004).
21. S.A. Mitchell, G. Randers-Pehrson, D.J. Brenner, and E.J. Hall. The bystander response in C3H 10T1/2 cells: the influence of cell-to-cell contact. *Radiat Res.* **161**, 397-401 (2004).
22. R. Baskar and P.U. Devi. Influence of gestational age to low-level gamma irradiation on

postnatal behavior in mice. *Neurotoxicol Teratol* **22**, 593-602 (2000).
23. M. Hossain and P. Uma Devi. Effect of irradiation at the early foetal stage on adult brain function of mouse: learning and memory. *Int J Radiat Biol* **77**, 581-5 (2001).

Published Paper and Abstracts Developed in this Project:

24. Gohlke, JM, Griffith, WC and Faustman, EM. 2005. *Computational models for the acquisition of neocortical neurons in the developing humans, monkey, and mouse: Cross species comparison of toxicodynamics*. Society of Toxicology Annual Meeting, New Orleans, LA. The Toxicologist. 84(S1): 69.
25. Gohlke Julia M.; Griffith Wifliani C.; Faustman Elaine M.2007. *Computational models of neocortical neuronogenesis and programmed cell death in the developing mouse, monkey, and human*. Cerebral Corttex 17:10, 2433-2442.
26. Griffith, WC, DeFrank, MN, Gohlke, JM, Gribble, EJ and Faustman, EM 2005a. *Systems biology models as a tool to integrate diverse studies of the developing neocortex after exposure to low dose radiation*. 42nd Congress of The European Societies of Toxicology. September 11-14, Cracow, Poland.
27. Griffith, WC, DeFrank, NM, Gohlke, JM, Gribble, EJ and Faustman, EM. 2005b. *Systems biology models as a tool to integrate diverse studies of the developing neocortex after exposure to low dose radiation*. Toxicology Letters. 158: S77-S77
28. Griffith, WC, Faustman, EM and Vigoren, EM. 2005c. *Quantitative models of bystander effects from ionizing radiation in non-targeted cells*. Society of Toxicology Annual Meeting, New Orleans, LA. The Toxicologist. 84(S1): 267
29. Griffith, WC, DeFrank, MN, Gohlke, JM, Gribble, EJ and Faustman, EM. 2006a. *Systems biology models for integration of diverse studies of the developing neocortex after exposure to low dose radiation from external and internal sources*. Society of Toxicology Annual Meeting, San Diego, CA. The Toxicologist. 90: 1641
30. Griffith, WC, Gohlke, JM, Vigoren, EM, Judd, NL, Lewandowski, TL, Bartell, SM, Defrank, NM, Ramprasad, J, Gribble, EJ and Faustman, EM. 2006b. *Conceptual framework for linking kinetic and dynamic process in quantitative models describing neurodevelopmental toxicology*. Epidemiology. 17(6): S152-S152
31. Griffith, WC, Yu, XZ, Nanspers, K, Dillman, JF, Ong, H, Vredevoogd, MA and Faustman, EM 2006c. *Systems biology evaluation of toxicogenomic microarray data using GO-Quant to analyze how toxicants alter gene pathways and functional gene categories*. Society for Risk Analysis Annual Meeting. December 3-6, Baltimore, MD.
32. Griffith, WC, DeFrank, MN, Gohlke, JM and Faustman, EM. 2007. *Value of information approach for development of models of the developing neocortex after exposure to low dose radiation from internally deposited radionuclides*. Society of Toxicology Annual Meeting, Charlotte, NC. The Toxicologist. 96: 1627

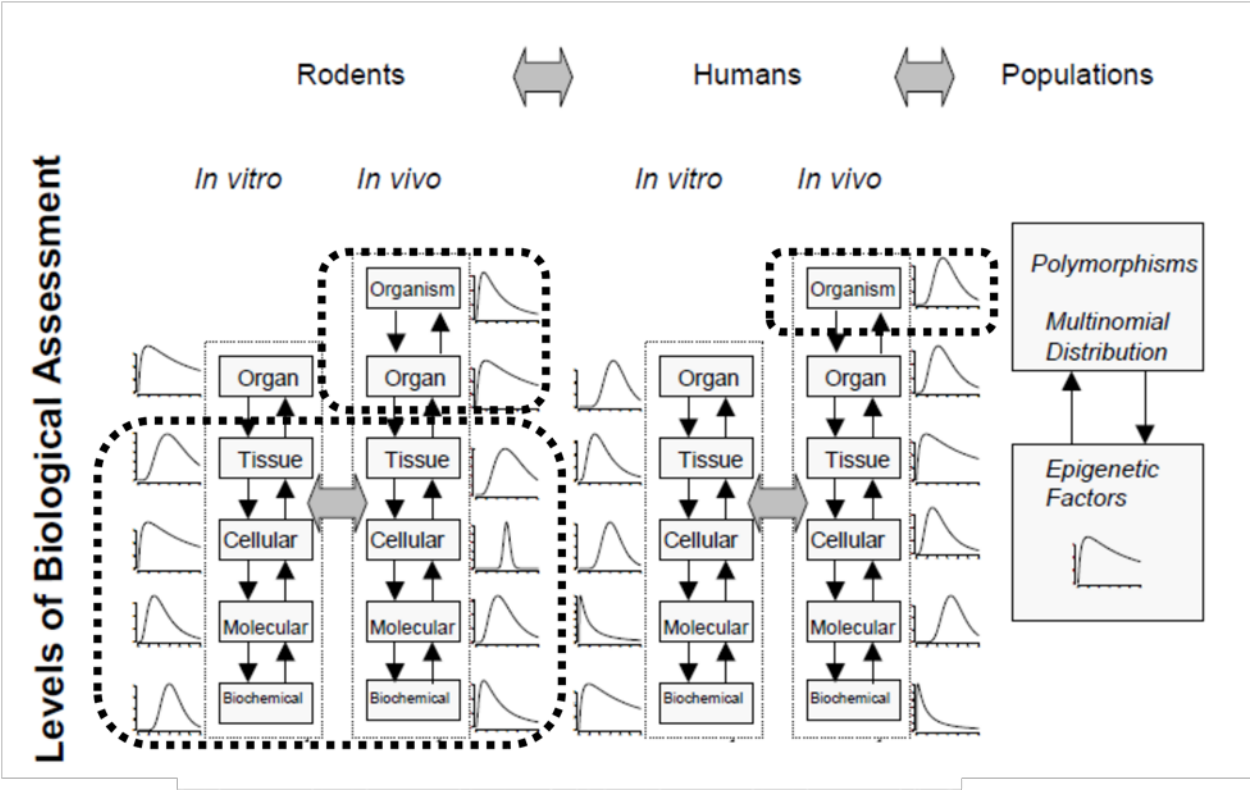

FIG. 1. Conceptual Model Framework: This multi-dimensional model framwork provides the structure used in this project in order to relate studies at multiple levels of biological organization to perform coss-species extrapolation from rodents to humans using in vitro and in vivo comparisons. The dashed boxes show the levels of Biological assessment and species for which we developed models.

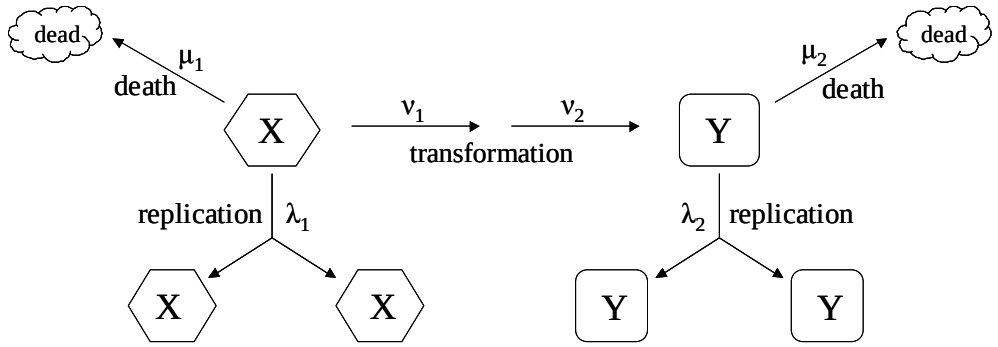

FIG. 2. Neuronal precursor cells (X cells) undergo three processes during neurogenesis: cell death (μ_1), replication (λ), and transformation (ν_1). X cells exiting the cell cycle become undifferentiated, migratory neurons (M cells) at a rate ν_1. M cells then transform into differentiated neurons (Y cells) once they cease migration at a biologically determined location. The rate at which cells transition from M cells to Y cells is represented by ν_2 and is dependent on the rate of movement along radial glial fibers (m) and the distance traversed during the migratory time period (d). Each cell population undergoes cell death at a rate μ.

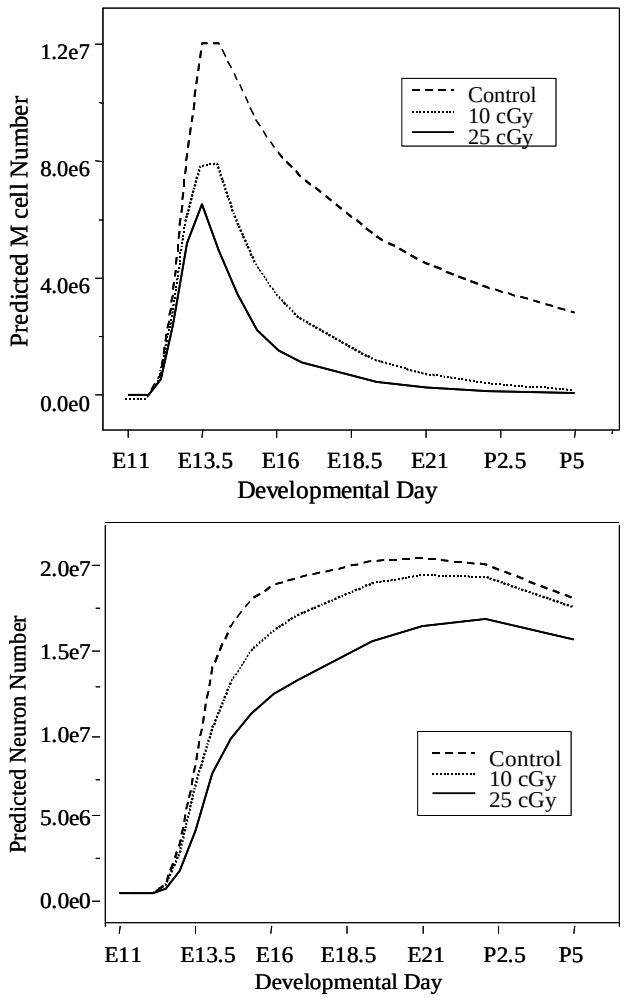

FIG.3. Model predictions for the effects of radiation on neuronal migration in the neocortex. A) Radiation causes a decreased rate of transformation of migrating neuronal cells (M) into differentiated neurons (Y) by slowing the process of migration and leading to sustained numbers of M cells. In the mouse, migration is expected to end by P5. B) In irradiated animals, migration continues into later development, as observed by the slower increase in Y cells.

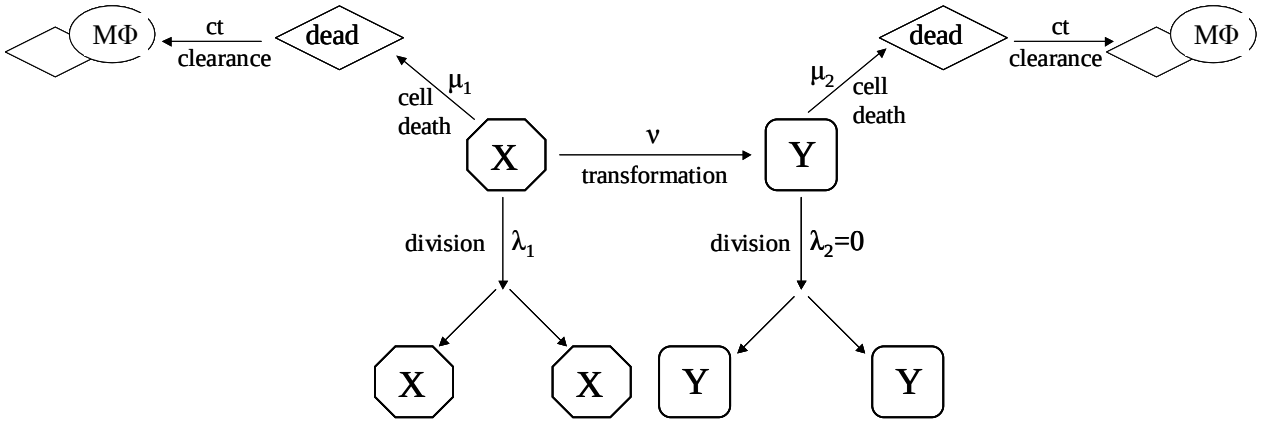

FIG.4. Model framework for Development (*21*). In this study, the model is applied to neocortex development. Type 'X' cells represent neuronal precursor cells in the proliferative regions. During each cell cycle, a precursor cell either stays in the proliferative region and undergoes further division (rate λ_1) or becomes a neuronal 'Y' cell (rate ν). Y cells are post-mitotic (rate $\lambda_2 = 0$). Both cell populations undergo cell death at unique rates (μ). Dead cells are removed from the population within some clearance time, ct.

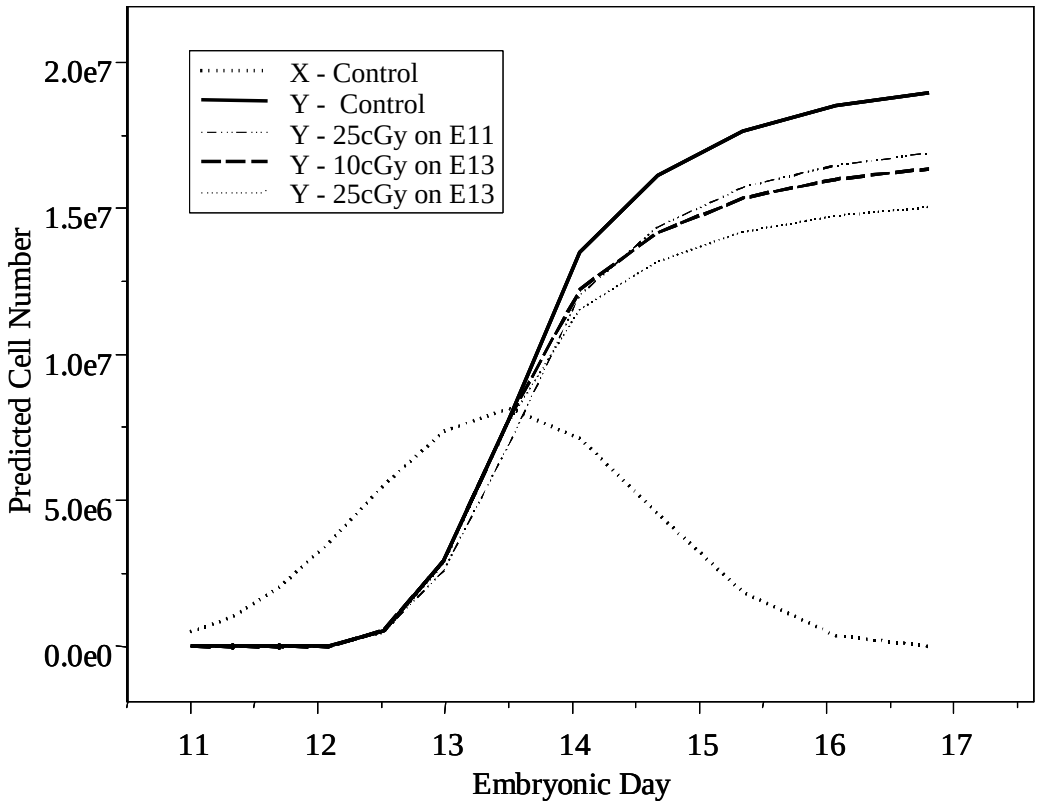

FIG. 5. Model predictions for the effects of radiation on cell death among neuronal precursors. The dose and time-dependent decrease of neuronal precursor cells following *in utero* irradiation leads to decreased neuron production.

TABLE 1

Behavior Studies[a] and Corresponding Model Predictions

Endpoint	LOAEL[b]	NOAEL[c]	Exposure	Reference	Y Cells[d] (% Control)
Locomotor activity	**25**	-	E14	Kimler & Norton 1988	95
	50	**35**	E11.5	Baskaret et al. 2000	89
Learning delay	50	**25**	E14	Hossain et al. 2001	95
	35	**25**	E11.5	Baskaret et al. 2000	90
Memory retention	50	**35**	E14.5	Baskaret al. 2000	94
	50	**25**	E14	Hossain et al. 2001	95
Exploratory activity	35	**25**	E12.5	Baskar et al. 2000	90

[a]Radiation-induced alterations in behavioral parameters across dose in young mice exposed to radiation *in utero* during neurogenesis.

[b]Lowest observable adverse effect level.

[c]No observable adverse effect level

[d]Model predictions, pertaining to improper migration following a NOEAL exposure on the treatment day, are included for comparison.

Appendix:

Models for the Effects of Low Doses of Radiation on the Developing Neocortex

INTRODUCTION

The developing brain is unique compared to other fetal organs for several reasons. The brain is especially complex in structure, with various regions and individual cells having specific identities and functions. Development of these regions is not synchronous, but takes place at specific intervals over various periods of time (*1*). Proper brain function is determined by the interconnection of various cells and structures. Normal structure depends on an orderly sequence of events, which must occur linearly in time and space *(2*). Lastly, central nervous system neurons cannot replicate, so alterations during development are often permanent and irreparable.

Due to its unique and complex structure and dependence on the specific timing of events, the developing neocortex is acutely sensitive to toxicant exposure (*3*). A wide range of chemical exposures, environmental conditions, and nutritional factors can have permanent deleterious effects on the developing brain. Radiation has been a thoroughly researched and well-documented neurological teratogen that can have significant effects on brain development (4). The most compelling effects were observed among the atomic bomb survivors. The most severely affected individuals were exposed between 8-15 weeks of gestation, a period of rapid replication of neuronal precursor cells and neuron differentiation (*5*). A clear dose- response relationship was observed in this population. Of those individuals exposed during this time to doses between 1-2 Gy, 62.5% were classified as mentally retarded and 29% were affected at a dose less than 1 Gy (*6*).

Low-dose exposures can cause less obvious effects, such as reduced learning ability and subtle behavioral differences. In the late 1950s, IQ tests were administered to many atomic bomb survivors who were exposed *in utero* to doses less than 50 cGy (*7*). Data on school performance in elementary school grades one through four also were collected. These data suggest that radiation exposure, especially exposures that occurred 8 to 15 weeks after conception, had a negative impact on both outcomes. For survivors exposed to a low dose (around 20 cGy), the loss of IQ was estimated to be about 5 points.

Radiation Effects on Migration of Neurons in the Neocortex

The developed mammalian neocortex is composed of six thin layers of neurons, each identified by the neuron type and the pattern of interconnections. After completing their last mitosis in the ventricular zone (VZ), cortical neurons undergo a long migratory process through

the intermediate zone (IZ, the future white matter) toward the cortical plate (CP, the future gray matter) (*8*). The complex pattern of neuron migration in the mammalian cerebral cortex has been termed 'inside-out'. As cells exit the cell cycle, the earliest formed neurons travel a short distance and occupy the deepest cortical layer (layer VI). Later-formed neurons must migrate past those generated earlier to occupy progressively more superficial layers. Thus, neurons forming layer I are formed last and must travel farthest, past the other five layers (*9*). Upon reaching a final location within the cortical plate, neurons differentiate and form functional units.

The primary mode of neuronal cell movement towards the cortical plate is migration along radial glial fibers. An audioradiographic analysis of migrating neurons in the murine neocortex estimated that 90-95% of migrating neurons in the IZ and lower CP contacted radial glial fibers (*10*). In comparison, most cells at the outermost regions of the CP had no contact with any radial glial fibers, indicating migration had stopped. Radial glial cells span the distance of the growing neocortex, with one short process extending to the VZ surface and a long process extending to the outer surface of the cortical plate (*11*). Neuronal migration along these fibers is modulated by cell-cell and cell-matrix interactions. These interactions activate signaling pathways between the radial glial cell and the migrating neuron, enabling cellular movement of the neural cell and maintaining the structure of the glial fiber (*12*).

Timing of the migratory process is crucial, as neurons must provide structural support for neighboring cells and be in the proper locations during synapse formation. If migration is slowed, neurons may not be able to form synapses with the correct neurons and the signal pathways can be impaired. Many toxicants and adverse environmental conditions have been shown to interfere with neuronal migration, either by affecting the migrating neuron or damaging supporting structures like radial glial cells. These toxicants include ionizing radiation (*13*), alcohol (*14*), cocaine (*15*), methylmercury (*16*), viral infections (*17*), and hyperthermia (*18*).

In humans, abnormal migration patterns or altered timing of migration have been implicated in a variety of neuropsychological problems, including fetal alcohol syndrome (*19*), schizophrenia (*20*), epilepsy (*21*), dyslexia and Tourette's syndrome (*22*). Similarly, animals treated with teratogenic agents shown to disrupt migration exhibit diverse neurological deficits. However, because of the non-specific mechanism of action (these agents also induce cell death and alterations in proliferation), these animal studies cannot provide conclusive evidence for the role of migration disorders in the development of neurological problems in humans.

Evidence of a migratory disorder following irradiation during neurogenesis (E11-17 in mouse) was first observed experimentally by Ferrer *et al*. (*23-24*), indicated by the presence of heterotopic neuron groupings. At high radiation doses, researchers observed a four-layer cerebral cortex that did not follow the normal 'inside-out' pattern of neuronal migration. These disruptions in neuronal migration have been attributed to three primary mechanisms: changes in the proteins responsible for locomotion, radial glial cell damage, or an alteration of the signaling pathways responsible for the cessation of migration (*25*). Each of these mechanisms has been implicated in the observed migratory effects of prenatal exposure to ionizing radiation.

The focus of this report is on disrupted neuronal migration due to radiation exposure and the structural and functional implications of these early biological effects. The cellular

mechanisms resulting in pathogenesis are most likely due to a combination of the three mechanisms mentioned. For the purposes of a computational model, quantitative studies of low dose radiation effects on migration of neuronal progenitor cells in the cerebral mantle of experimental animals were used.

Death of Neurons Caused by Radiation in the Developing Neocortex

Radiation exposures that cause mental retardation, reduced learning ability and subtle behavioral differences we hypothesize are also due to an aberrant loss of neuronal precursor cells or inappropriate cell death among post-mitotic neuronal cells in the developing brain, which can result in a decreased neuron number in the mature brain (26, *27, 28*). Considering that a single precursor cell present at E11 in the mouse is estimated to contribute over 250 neurons to the final population (29), cell death of these early cells due to toxicant exposure can have a substantial impact on neuron production. Various toxicants have been shown to result in decreased neuron number through the induction of apoptosis in neuronal precursor cells or post-mitotic neurons following an exposure during neurogenesis, including radiation (30), methylmercury (31), and ethanol (32).

Excessive apoptosis can also result from the pathogenesis occurring in many acute and chronic neurological disorders. Following an acute brain injury, such as trauma, spinal cord injury, and ischemic stroke, massive cell death can be observed in localized areas of the brain. Chronic disease states such as Alzheimer's, Parkinson's, and Huntington's diseases, amyotrophic lateral sclerosis, spinal muscular atrophy, and diabetic neuropathy are also related to the loss of specific neuron populations (33). Among persons with developmental disorders, including schizophrenia and autism, deficits in neuron number have been observed (34). Alternatively, inhibition of normal apoptosis during synaptogenesis, in which up to half of the neurons generated are eliminated, can result in the retained presence of neurons that should have been removed from the neuron population (*3*). Therefore, any alterations in the normal apoptotic activity or proliferative events in the developing nervous system can lead to an incorrect number of mature neurons.

Extensive research on how environmental exposures can alter proliferation and apoptosis in the developing brain is under way. It is known that exposure to ionizing radiation can cause nuclear and mitochondrial DNA damage, which is mediated by the increase in reactive oxygen species (ROS). The ROS generated by radiation exposure has been shown to activate apoptosis signaling pathways and halt cell cycle progression in proliferating neuronal precursor cells (35). Radiation-induced cell death among proliferating cells in the rodent neocortex occurs at doses as low as 10 cGy (36). At these low doses, cells die via apoptosis, as determined by the observed molecular features characteristic of this mode of cell death, including loss of cell processes, smooth cell surface, cell shrinkage, and chromatin condensation (37). Low doses of radiation (50 cGy) have also been shown to be anti-inflammatory in macrophages (38). Higher doses (>1 Gy), however, lead to necrotic cell death with macrophage activation and cytokine release, triggering inflammation in the damaged neocortex.

Researchers have used a variety of molecular markers to evaluate cell death in the radiation-exposed developing brain, including DNA laddering (39), hemotoxyln and eosin

staining to identify pyknotic nuclei (40), and mRNA quanitification of pro- and anti-apoptotic gene expression (39). Bolaris et al. (41) demonstrated that apoptosis of neuronal precursor cells was specifically associated with the up-regulation of p53. Following *in utero* irradiation on E17 or E14, cells in the developing rat neocortex were assessed for p53 stabilization by immunocytochemistry and apoptotic nuclei by TUNEL staining. Histological evidence demonstrated that all TUNEL-positive cells were also p53-positive, while approximately half of the p53-positive cells are also TUNEL-positive. Thus some pathway-specific information is available on essential cell signaling pathways.

Dying cells are typically removed by macrophage phagocytosis. The unexposed neocortex has very few macrophages during this developmental time period. Morphological analysis of the rat neocortex after irradiation on E15 shown that the number of macrophages in the proliferative regions was increased compared to controls (42). This influx of macrophages increased with time and peaked at 30 hours after exposure. Researchers noted that vesicles containing fragmented nuclei were present in the macrophages at the 12 and 24-hour time points after exposure. Likewise, the number of pyknotic cells in the neocortex decreased at these time points, presumably a reflection of the disappearance of dead cells by phagocytosis. It is unknown as to whether the influx of macrophages is the result of recruitment of circulating macrophages from outside the brain region or from a premature damage-induced differentiation of microglia. Highlighting the importance of dead cell clearance, it has been suggested that the retention of dead cells may contribute far more to the development of postnatal effects than actual reduction of cell number (43).

Many studies have demonstrated that extensive cell death is induced in the developing murine cerebral cortex within a few hours after radiation exposure. Surviving fetuses typically have abnormal behavior patterns and deficits in neurological function (44). Therefore, it is hypothesized that neural cell death is a primary component in the radiation-induced abnormal development of the mammalian brain. This portion of the computational model that we developed aims at quantitatively determining how radiation-induced cell death of neuronal precursor cells affects the number of post-mitotic neurons at the end of the neurogenesis period.

Models of Radiation Effects on Neuron Migration and Death in the Neocortex

Neuron Migration Model Framework

The basic framework for this developmental model was adapted from the model of Leroux *et al*. (*45*), which describes organogenesis through the processes of cellular replication, differentiation, and death (Figure 1). The model defines X cells as neuronal precursor cells. Each X cell can replicate and form two X daughter cells or differentiate into a post-mitotic neuron, Y cell. The model can be modified to accommodate replication events that produce one X cell and one Y cell. The X cell replication rate (λ) and the transformation rate (ν) are time dependent. Both X and Y cells undergo cell death at a specified background rate (μ). Replication and differentiation rates for X cells, corresponding to neuronal precursor cells in the fetal mouse, are incorporated from published literature. The division rate of Y cells is set to zero to simulate a terminally differentiated status.

To simplify the mechanism of neuronal migration, the framework for the migration model is summarized as follows: neuronal precursor cells (X cells) exit the cell cycle and become undifferentiated, migratory neurons (M cells). M cells then transform into differentiated neurons (Y cells) once they cease migration at a biologically determined location. The rate at which cells transition from M cells to Y cells is represented by ν_2. Various mechanistic data for the effects of radiation can be incorporated into this ν rate.

Cell division. The time dependent control rates for replication (λ), transformation (ν), and cell death (μ) were determined for the mouse neocortex during the period of maximum sensitivity to radiation exposure, from embryonic day 11 (E11) to postnatal day 5 (P5). This time period encompasses the eleven cell cycles of neurogenesis, which occurs from E11-E17. These rates were calculated from previously published data (*46*). Replications rates are based upon a 5-bromo-2'-deoxyuridine (BuDR) study by Takahashi *et al*. (*47*), in which neuronal precursor cells were labeled with BuDR during the S-phase of mitosis. From these labeling experiments, the length of the cell cycle (T_c) can be determined. The cell cycle length and the replication rate are related by the following equation:

$$\lambda = LN(2)/T_c \quad (1)$$

The data demonstrate that the cell cycle length of precursor cells increases across the eleven cell cycles. Correspondingly, the rate of replication decreases throughout neurogenesis. Refer to Golkhe *et al*. (*46*) for a detailed explanation of this parameter.

Cell death. Control death rates for both X and Y cells were based on the following equation:

$$\mu = -[LN(1-(\%TUNEL+)/100)*24]/2.5 \quad (2)$$

where the percent of cells in the neocortex that were TUNEL-positive was estimated from studies using terminal transferase dUTP nick end labeling (TUNEL) of apoptotic cells. Haydar *et al*. (*48*) reported that the percentage of apoptotic cells in the murine neocortex from E14 to E18 was relatively constant at 0.14%. Similarly, Hoshino *et al*. (*49*) observed a constant percentage of dead cells in the ventricular zone (0.2%) across neurogenesis. For reasons of consistency with the radiation datasets, the Hoshino data was used to calculate the control death rate among X cells (μ_1). In calculating the death rate, the clearance of dead cells was assumed to occur within 2.5 hours based on a study by Thomaidou *et al*. (*50*).

The rate of cell death among Y cells (μ_2) was determined for the postnatal period, until P5, when migration ends. This death rate is based on the percentage of TUNEL+ neurons in the murine neocortex. During the prenatal period, normal cell death among neurons is rare, and Verney et al. (51) determined that only 0.05% of cells are dying. However, researchers observed an increase to 0.9% on P5. Refer to Golkhe *et al*. (*52*) for a detailed explanation of this parameter.

Quantitative Modeling of neuronal migration

A model schematic is presented in Figure 1. In this model framework, we have assumed that neuronal cells become differentiated neurons once migration has finished. The transformation parameters are composed of two rates: the rate at which neuronal precursor cells

exit the cell cycle (ν_1) and the rate at which migratory neuronal cells become differentiated neurons (ν_2).

Cell cycle exit. Transition from the proliferative neuronal precursor cell (X) to a post-mitotic migratory neuronal cell (M) is described by the rate ν_1. This rate of cell cycle exit was determined from data generated by Takahashi *et al*. (*53*). In this model, cells that continue to undergo replication represent the P fraction (proliferative fraction) and cells that exit the cell cycle constitute the Q fraction (quiescent fraction). In this model, the Q fraction is indicative of migratory neuronal cells *en route* to the cortical plate. The Q fraction was estimated from double labeling studies of BuDR and tritiated thymidine (^{3}H-TdR) incorporation into S-phase cells. X cells continue to be generated across eleven cell cycles, which occupies approximately seven embryonic days in the fetal mouse (E11 to E17). However, the fraction of cells that reenter a new cell cycle decreased with time during neurogenesis. Correspondingly, the Q fraction steadily increases across neurogenesis until all neuronal precursor cells have exited the cell cycle (after the eleventh cell cycle) and the P fraction reaches zero. At the end of each of the eleven cell cycles, the Q fraction can be determined:

$$Q = M(t)/[X(t) + M(t)] \quad (3)$$

where X(t) and M(t) indicate the number of precursor cells and post-mitotic, migratory neuronal cells at time t. Figure 2.A provides the ν_1 rate information generated from this data set.

Migration parameters. The second component of the transformation model describes the rate at which cells stop migration and occupy a final position at the outer layers of the growing cortical plate. This rate, ν_2, is derived from two parameters: the rate of cell movement along radial glia fibers (m) and the migratory distance required (d). The rate of neuronal migration (m) was determined in several studies by a variety of experimental approaches. Miller (*54*) and Takahashi et al. (*53*) estimated the rate of neuronal migration by labeling cycling cells during neurogenesis and measuring their locations in the cortical plate several days later. Miller labeled cells in the fetal rat with ^{3}H-TdR on E15, 17, 19, and 21. This distance traveled in two days was used in estimating the rate of migration, 5 μm per hour. Using fetal mice, the Takahashi group employed a similar protocol and estimated the average migration rate to be 5.1 μm per hour.

In vitro systems were also utilized in determining the rate of neuron migration by measuring cell movement along radial glia fibers. Adams *et al*. (*55*) and Edmondson *et al*. (*56*) used time-lapsed video microscopy to observe neurons traveling along the radial glial fibers. Purified granule neurons and astroglia were isolated from neonatal mice and cultured for 48-72 hours. Time and distance measurements were obtained in addition to a detailed qualitative analysis of the migratory process. Anton *et al*. (*57*) employed a cortical imprint assay with sections from the E18 murine neocortex. This assay isolates radial glial cells with migrating neurons attached to them. The changing location of the neuronal cell body was divided by time elapsed between observations (5-15 minutes) to calculate the migration rate of 10.1 μm/hr. Seeds *et al*. (*58*) sectioned the cerebellum of mice on postnatal day 8 (P8). This is the time of most rapid migration in the cerebellum. In culture, neurons were labeled with DiI and observed at 20-30 minute intervals for movement along Bergmann glia cells (analogous to radial glial cells in the cerebral cortex). Migration rate was calculated at 7.3 μm/hr. Table 1 contains a summary of these migration studies.

The other parameter determining the ν_2 rate is the migratory distance. Over the course of neuron migration, the cortical plate expands several fold. The length of the radial glial fiber grows in relationship to this cortical expansion. Therefore, the distance neurons have to migrate, in order to occupy progressively superficial layers, increases across the developmental time period (*57*). Takahashi et al. (*53*) measured the thickness of the neocortex, from the VZ to the outer boarder of the cortical plate, across the eight days of neurogenesis. Neuronal migration ends in the neonatal mouse at postnatal day 5 (P5). The thickness of the neocortex on P5 is 716 μm (*59*), which is assumed to be the maximum distance traversed by a migrating neuron. Figure 2.B depicts the neocortical measurements from these studies. A loess regression line has been applied to these data. The rate at which M cells stop migrating and differentiate into Y cells (ν_2) is assumed to occur exponentially. Under this assumption, the ν_2 rate is related to the average migration time by the following equation:

$$\nu_2 = LN(2) / \text{migration time} \quad (4)$$

where the average migration time is calculated from the migratory rate (m) and the neocortical thickness at each time point. Uncertainties in the ν_2 rate are due to the different experimental measurements of the migratory rate, m. Upon exposure to ionizing radiation during critical times of neurogenesis, ν_2 is altered and leads to significant alterations in the process of neuronal migration.

Radiation effects on neuron migration. For the purpose of computational modeling, a dataset generated by Fushiki *et a.l* (*60*) was used in determining the quantitative effects of radiation on neuronal migration. Investigators studied the effects of a low-dose radiation exposure on the migration of neurons from VZ towards the cortical plate in mice during the period of rapid neuron migration. Pregnant Wistar rats received intraperitoneal injections of tritated thymadine (^{3}H-TdR) on E16 of pregnancy to label S phase cells. One hour later, the animals were irradiated with a single dose (between 5 and 20 cGy) of γ-rays from a ^{60}Co-source. On E18, evaluation of neuronal migration was performed by autoradiography. The dorsolateral portion of the neocortex was divided into four sections (VZ, inner IZ, outer IZ, and CP) and the percentage of heavily labeled cells per section was determined.

In the control animals, the percent distribution of cells in the neocortex two days after irradiation indicated that 22% of labeled cells were in the CP region. Similar distributions were observed two days after irradiation in the 5 and 10 cGy treatment groups, indicating a possible threshold for this effect. In comparison, only 13% and 8% of labeled cells had reached the CP in the 15 and 20 cGy treatment groups respectively. These treatment groups also exhibited an accumulation of labeled cells in the VZ, with 41% and 47% of cells remaining in the proliferative region (compared to only 27% in control brains). From this data set, we can determine how radiation affects the migration rate of post-mitotic neurons. Assuming that the migratory process is described by an exponential rate, we can assess these effects by the following equation:

$$Y(t) = Y_o * \exp(- c * m * t) \quad (5)$$

where Y(t) is the percentage of post-mitotic cells that have reached the CP at a specific time (48 hours in this case). The c term is a constant and Y_o is the percentage of cells that reach the CP in control animals. In solving this equation for m, we can describe the effects of radiation on migration. Alterations in the m rate are dose-dependent. Linear and polynomial fits to the data

were applied. The polynomial fit was considered to be more accurate in terms of incorporating a threshold. We assumed that the average distance migrated by a neuron (d) during each time point does not differ compared to control brains. The dose-dependent ν_2 rates were calculated (Figure 2.C) and incorporated into the neurogenesis model to determine the number of neurons that have reached their final position within the CP following a radiation exposure.

Neuron Death Model Framework

To computationally model the development of the neocortex and determine how toxicant exposure affects development, three major processes are described:

1. Replication of neuronal precursor cells
2. Transformation of neuronal precursor cells into differentiated neurons
3. Cell death among the X and Y cell populations

The basic framework for this developmental model was adapted from the model of Leroux *et al*. (*45*), which describes organogenesis through the processes of cellular replication, differentiation, and death. Our model defines X cells as neuronal precursor cells. Each X cell can replicate and form two X daughter cells or differentiate into a post-mitotic neuron, Y cell. The X cell replication rate (λ) and the transformation rate (ν) are time dependent. Both X and Y cells undergo cell death at a specified background rate (μ). Replication and differentiation rates for X cells, corresponding to neuronal precursor cells in the fetal mouse, are incorporated from published literature. The division rate of Y cells is set to zero to simulate a terminally differentiated status.

The current computational model focuses on the neocortical effects following low doses of radiation. Under normal conditions the death rate (μ) is very low for X, M, and Y cells. This model focuses on the effects of radiation on neurogenesis, with emphasis placed on the effects on X cells. Surviving X cells continue to proliferate and it is assumed that replication proceeds at control rates. In modeling radiation-induced cell death within the neocortex, the neurogenesis model was expanded to incorporate the decreased capacity of dead cell clearance following an acute low-dose exposure.

Description of Parameters for Neuron Death

The time dependent differential equations are used to describe the control rates for replication (λ), transformation (ν), and cell death (μ), which were determined for the mouse neocortex during the period of maximum sensitivity to radiation exposure (E11-E17). This time period encompasses the eleven cell cycles of neurogenesis. These rates were calculated from previously published data (*46*) and the parameters used in the calculations of these rates are summarized in Table 2. The cell cycle length (T_c) and the replication rate are related by equation 1.

Transition from the proliferative neuronal precursor cell (X) to a post-mitotic neuronal cell (Y) is described by the rate ν. It is assumed that precursor cells adopt neuronal characteristics following cell cycle exit. At the end of each of the eleven cell cycles, the Q

(quiescent) fraction, which is the proportion of X cells that have exited the cell cycle, can be determined:

$$Q = Y(t)/[X(t) + Y(t)] \quad (6)$$

where X(t) and Y(t) indicate the number of precursor cells and post-mitotic neurons at time t. The initial number of X cells (X_o) was estimated from a stereological examination of the murine neocortex on E11 (*47*).

Controlled cell death plays an important role in brain formation during later neurodevelopment, when approximately half of the post-mitotic neurons produced will die via apoptosis (*2*), but apoptosis in the early stages of development is rare. Calculations of the death rate among the X and Y cell populations is based on the percentage of dying neurons in the murine neocortex. Control death rates for both X and Y cells were based on equation 2 where the percent of cells in the neocortex that were dying was estimated from studies using terminal transferase dUTP nick end labeling (TUNEL) of apoptotic cells or cells with pyknotic nuclei. The time to clear dying cells, ct, is affected by radiation. In terms of quantifying the rate of cell death, this information is important for determining how long a dying cell can be observed and is proportional to the ratio of pyknotic cells per macrophage. In conjunction with the ratio of macrophages per pyknotic cells, the average clearance time following irradiation can be determined as a function of the dose. Prior to exposure and after the 24-hour period of observation, the control clearance time of 2.5 hours was used.

The selected doses used in this model were chosen because of the subtle structural and functional effects caused when exposure occurs during the time of neurogenesis. These low doses encompass exposures less than 50 cGy and do not elicit an inflammatory reaction. High dose exposures could be modeled with the addition of parameters pertaining to induced inflammation and necrotic cell death.

Experimental Data Evaluation for Death of Neurons

Replications rates are based upon a 5-bromo-2'-deoxyuridine (BuDR) study by Takahashi *et al*. (*47*), in which neuronal precursor cells were labeled with BuDR during the S-phase of mitosis. From these labeling experiments, the length of the cell cycle (T_c) can be determined. The data demonstrate that the cell cycle length of precursor cells increases across the eleven cell cycles. Correspondingly, the rate of replication decreases throughout neurogenesis. Refer to Golkhe *et al*. (*46*) for a detailed explanation of this parameter.

This rate of cell cycle exit, ν, was determined from data generated by Takahashi *et al*. (*53*). In this model, cells that continue to undergo replication represent the P fraction (proliferative fraction) and cells that exit the cell cycle constitute the Q fraction (quiescent fraction). The Q fraction was estimated from double labeling studies of BuDR and tritiated thymidine (^{3}H-TdR) incorporation into S-phase cells. X cells continue to be generated across eleven cell cycles, which occupies approximately seven embryonic days in the fetal mouse (E11 to E17). However, the fraction of cells that reenter a new cell cycle decreased with time during neurogenesis. Correspondingly, the Q fraction steadily increases across neurogenesis until all neuronal precursor cells have exited the cell cycle (after the eleventh cell cycle) and the P fraction reaches zero.

Many studies have observed minimal cell death in the growing mammalian brain during neurogenesis. Under control conditions, several studies have estimated the percentage of dead cells to be low among proliferating neuronal precursor cells (X cells) (37, *40*, *53*) according to both the TUNEL assay and pyknotic counts. Haydar *et al*. (*48*) reported that the percentage of apoptotic cells in the murine neocortex from E14 to E18 was relatively constant at 0.14%. Hoshino *et al.* (40) report a similar percentage (0.2%) of cells in the proliferative regions as pyknotic . For reasons of consistency with the radiation datasets, the Hoshino data was used to calculate the control death rate among X cells (μ_1).

Increased rates of cell death following irradiation were determined from the Hoshino *et al.* (40) study. Pregnant mice were treated with a single exposure at a dose of 3, 6, 12, 24, or 48 cGy of γ-rays on E10, 13, or 15. Fetuses were removed, sections of the neocortex were stained with hemotoxylin and eosin, and pyknotic cells in the VZ were counted within 24 hours after exposure. The neocortex consisted only of the VZ on E10, and these counts were assumed to represent irradiation on E11 in our model. Results from this model show that cell death peaks between 6 and 9 hours after a single radiation exposure. Irradiation on E13 caused the highest percentage of pyknotic cells (13.2%) and exposure on E15 had the least effect (4.5%). It is hypothesized that this differential sensitivity is related to the rate of replication at the time of exposure, with cells that are replicating at a faster rate demonstrating an increased rate of cell death.

To assess this altered clearance time, a data set by Kimler (43) was used in comparing the influx of macrophages into the neocortex compared to the increase in pyknotic cells. A positive correlation between the number of pyknotic cells and the influx of macrophages into the neocortex developed with time after an acute exposure, with doses ranging between 6 and 100 cGy. Licht *et al.* (61) estimated the clearance capacity of a single macrophage using an *in vitro* assay. Murine thymocytes were isolated and treated with dexamethasone for three hours to induce apoptosis (this was assessed by Annexin V reactivity, which is an early indicator of apoptotic cell death). Macrophage cells were incubated with these apoptotic cells and the average uptake of dead cells by one macrophage was 5 per hour. In determining the ct for our neocortical model, we assumed this maximum rate was constant across all times and doses.

Based on the Hoshino *et al*. (40) and Kimler (43) data, the rates of cell death were determined for the 24 hours following *in utero* exposure. Data shows that the increase in cell death is transient and returns to control levels by 24 hours after exposure (42, *61*). This applies only to low doses, since higher exposures result in sustained apoptotic levels. For example, a 2 Gy exposure resulted in increased apoptosis up to 48 hours after exposure (63). The Hoshino *et al.* (*40*) data set examines only those cells in the proliferative regions of the neocortex. Therefore, we assume that this death rate applied only to X cells (μ_1). The effect of radiation on Y cell death (μ_2) was not modeled; as we have assumed this post-mitotic cell population is radio-resistant.

Results And Discussion Of Models

Control Model for Neuron Migration in the Neocortex

Post-mitotic neuronal cells (M cells) that are generated in the first few rounds of replication will transform into differentiated neurons at a fast rate because the distance from the VZ to the CP is short. M cells generated towards the end of neurogenesis will transform into Y cells at a slower rate because their final destinations, at the superficial layers of the CP, are relatively distant. Based on these rates, the number of M cells that have reached their final destination can be calculated. Once these cells stop migrating, they are considered to be differentiated neurons, or Y cells. Figure 5 shows the model predictions for the number of Y cells in the control brain. The simulation was run until postnatal day 5, which marks the end of the migration period in the mouse neocortex (*1*).

Prior to the incorporation of migration into the computational framework, the model predicted that 21 million differentiated neurons (Y cells) would be generated by E18 in the murine neocortex (Figure 5). However, neuronal migration in murine neocortex continues past E18. In this migration model, under the assumption that post-mitotic neuronal cells (M) move along radial glial fibers at a constant rate, the transformation process is lengthened to incorporate this sensitive time period of neurodevelopment.

Model predictions were compared to stereological estimates of neuron production in the murine neocortex. After accounting for 50% cell loss due to normal neuron death during postnatal development, estimates based on neuron number in the adult murine neocortex show approximately 10,500,000 (*64*) and 12,700,000 neurons (*65*) respectively. After incorporation of the migratory process into the computational model, predictions are slightly more approximate to the stereological estimates compared to the original model, however both models predict greater neuron number than the stereological estimates.

Variations in the migratory rate (m) of neurons along radial glial fibers (see Table 1) do not lead to differences in the number of neurons produced, but do affect when migration ends. For example, if the m rate of 33 μm/hr is used (*56*), the model predicts that all M cells will differentiate into Y cells by E20, versus P2 when the value of 10.1 μm/hr is used (*57*). For simplicity, the control rate determined by Anton *et al*. (*57*) is used throughout the rest of this analysis when assessing the impact of radiation on neuronal migration. This migration speed was used because mouse brains from E18 embryos (a time of maximum migratory action) were employed in this model. The other studies focused on later developmental times or used cerebellum cultures. Additionally, cell movement was monitored every five minutes for up to six hours in the Anton et al. study. This monitoring schedule was more rigorous than the other studies.

Radiation Model

Animal research has shown that post-mitotic neuronal cells tend to accumulate in the VZ and IZ following a radiation exposure (*66*, *67*). In these studies, the number of post-mitotic neurons in the neocortex was not significantly different than that of the control brains in the days following exposure. However, their distribution among the cortical regions was apparent, with fewer post-mitotic neuronal cells reaching the cortical plate. Our model quantitatively predicts the effect of radiation on neuron differentiation based upon changes in the migration rate of these neuronal cells.

According to the model, upon radiation exposure at the beginning of neurogenesis (E11), the transformation of post-mitotic neuronal cells (M) into neurons (Y) is slowed. The decreased

transition rate (ν_2) is due to a slower migration of M cells. In a dose-dependent manner, M cells accumulate in the neocortex (Figure 6.A). Likewise, the number of Y cells does not peak until later in development (Figure 6 B). A 10 cGy exposure does not lead to major alterations in the growth of the Y cell population. At P5, the day when all M cells complete migration in control brains, the exposed brain has only 2.5% of its M cells still migrating. According to our predictions, these remaining 50,000 cells would complete migration within two days, or by P7. A 25 cGy exposure leads to a 75% decrease in the rate of transition between M cells and Y cells (ν_2). This leads to a sustained presence of migrating cells, M, in the neocortex. Y cells may eventually reach control levels, but it would require an additional 25 days for this to occur.

The incorporation of neuronal migration adds valuable information to our model of neurogenesis. This process is highly susceptible to toxicant exposure and alterations in migration have been associated with several pathological manifestations (*11*). If we assume that post-mitotic neuronal cells immediately adopt the identity of a differentiated neuron, predictions of Y cell numbers escalate too quickly (Figure 5) and the susceptibility of the migration process cannot be assessed. Through the incorporation of parameters describing neuronal migration, we can more accurately assess how toxicants affect neurodevelopment. The model can also be used to predict relative neuron position in addition to neuron number.

Many studies have shown that ionizing radiation disrupts neuronal migration. Data from Fushiki *et al*. (*60*), which indicate that neurons exposed to radiation reach the cortical plate at a slower rate, were used in quantifying these migratory effects. Neuronal migration in the mouse is expected to end on P5 (*1*). According to model predictions in the control brain, 20,600,000 Y cells have been formed by this time. Upon exposure to 10 cGy of radiation, differentiated neuron production drops by only 3% on P5. Y cells could potentially reach control values by P7, only two days after migration should have ended. Higher doses of radiation lead to more significant alterations in the pattern of neuron production. Model predictions show that a 25 cGy exposure will result in only 87% of post-mitotic M cells having reached their final locations by P5 (Figure 6.C). The model predicts that migration would be complete by P30, a hypothetical 25-day extension of the migratory process, if allowed to continue normally.

Alternatively, it is likely that neuronal migration does not continue into later development (i.e. past P5), and neurons will terminally differentiate in inappropriate locations. Premature differentiation is observed in animals exposed to higher doses of radiation (>50 cGy) with the formation of neuronal heterotopia (*66*). However, induction of heterotopia has not been observed in low-dose treated animals. Other researchers have concluded that the aberrantly located neurons will not continue migration, but will undergo apoptosis during postnatal development. Based on this possibility, if we assumed that improperly located neurons on P5 died, our model would predict a 3% and 13% loss of neurons following doses of 10 and 25 cGy respectively (Figure 6.C).

Studies examining long-term effects of radiation on neuron migration were used to validate model predictions. In a follow-up study by Fushiki *et al*. (*68*), the effects of radiation on neuronal migration were examined later in development. Pregnant mice were irradiated with 10-100 cGy on E14 and the movement of BrdU-labeled cells through the different layers of the cerebral cortex was followed. The relative positions of labeled cells were altered in all radiation-treated groups, compared to control brains, during postnatal weeks 2 and 3. At these time points,

neuronal migration in the control brains has ended. Results show a decreased percentage of cells in cortical layer IV and an increased percentage of cells in layers II/III in irradiated mice. Specifically, results show 10% of the labeled cells are not in a proper location during weeks 2 and 3 following a 25 cGy exposure. In comparison, predictions from our model also indicate that 13% of neuronal cells will have inappropriate locations at P5, but this percentage will drop to only 2% by week 3, if migration is assumed to continue normally after P5.

Further examination by Fushiki *et al*. (*68*) at postnatal week 8 shows no significant differences in the distribution of labeled cells across the six cortical layers. In comparison, our model predictions indicate that animals exposed to 10 cGy of irradiation would have normal cell distributions much earlier (by postnatal week 1), and a 25 cGy exposure would lead to normal distribution patterns by week 4. However, this conclusion is based on the assumption that neurons can continue the migratory process during these later stages of neurodevelopment until normal positions can be reached. An alternative explanation is that aberrantly situated cells within the neocortex are more likely to undergo apoptosis. Based on this assumption, model predictions are presented as the number of neuronal cells that have properly migrated by P5, with all remaining M cells undergoing apoptosis (Figure 6.C).

In a similar study by Inouye *et al*. (*67*), an abnormal distribution of labeled cells in the mouse neocortex was still observed during postnatal week 6 following a 24 cGy exposure on E16. Researchers observed a greater percentage of cells occupying layers V and VI, with fewer labeled cells in layers II/III. Later time points are not examined in this study. Compared to our model estimates, this study indicates that migration is slowed to a further extent than predicted by our model.

Overall, these studies do support the current predictions of our model, in which radiation exposure results in a disorganized neuronal cytoarchitecture in the postnatal neocortex. Postnatal neurodevelopment in the mouse includes synaptogenesis, and the presence of irregularly placed neurons can lead to failed connections or misconnections between neurons. We conclude that this abnormal cytoarchitecture within the developing neocortex is the basis for some of the neurobehavioral and intellectual deficits observed in animals and humans prenatally-exposed to ionizing radiation and other toxicants.

There is a lack of comparable estimates of neuron production following *in utero* irradiation at low doses in rodent models, however comparison of the model output to behavioral endpoints can be informative. Table 3 displays the no observable adverse effect level (NOAEL) and the lowest observable adverse effect level (LOAEL) for behavioral effects in mice exposed to low doses of radiation during neurogenesis. Baskar & Uma Devi (*69*) determined that learning delays, assessed by the hole board test, were present in animals exposed to 35 cGy on E11.5 and E12.5. According to our model predictions, this corresponds to 10% of neuron improperly located within the neocortex on P5. Animals exposed on E14.5 did not demonstrate a learning delay until the exposure reached 50 cGy, related to a 5% reduction in neurons. Exposure on E17.5 did not affect learning behavior, and our model predicts very small decreases in neuron production after exposure at this time. A second study by Hossain & Uma Devi (*70*) determined the NOAEL for memory retention was 25 cGy when exposure occurred on E14. Model predictions indicate that 5% of post-mitotic neurons would be improperly located on P5.

The process of neuronal migration along radial glia can be described in three steps. First, the differentiated neuron must express specific binding proteins on its cell surface and bind to the glial fiber. Second, the neuron traverses a specific distance, up to the entire length of the glial fiber. Lastly, the neuron detaches from the glial fiber at a biologically determined location. Therefore, the parameters that could potentially determine the number of migrated neurons include the number of radial glial cells, binding affinity of the neuron to the glial cell, rates of migration, times of migration, and the location of detachment from the glial fiber. In animal studies, radiation has been shown to affect each of these parameters.

Currently, our model does not make any assumptions as to the exact mechanism of migration disruption following irradiation. More detailed information pertaining to migratory disruption, such as dose-response data for damage to radial glial fibers or changes in protein expression, can easily be incorporated into the model. This information would provide insight into toxicant-specific mechanisms and enable the use of more *in vitro* data in our developmental dose-response model. Future developments of this model include the addition of this detailed information into the model in order to gain a better understanding of normal neuron migration and how toxicant exposure alters this sensitive process.

Neuron Death Model Results and Discussion

The basic neurogenesis model was expanded to incorporate changes in cell death rates caused by radiation exposure in utero. The model framework is shown in Figure 3, in which the dose-dependent parameter of clearance time, ct, is added to better describe radiation-induced cell death processes. Based on the Hoshino study (40), the control death rate for X cells is 2e-5 per hour and this rate was assumed to be constant across neurogenesis. In calculating the death rate, the clearance of dead cells was assumed to occur within 2.5 hours based on a study by Thomaidou *et al*. (*50*). All model rates in the unexposed murine neocortex were calculated from experimental data and are summarized in Figure 4.

Rapid increases in the number of dying cells were observed experimentally (40) following a single low dose exposure, which overwhelms the clearance capacity of dead cells during this developmental period. Upon radiation exposure, the rate of cell death increases, as the clearance time increases. Figure 7 illustrates the dose and time-dependent effects on the cell death rate among neuronal precursor cells (μ_1).

Reduction in neuron production following a radiation exposure during neurogenesis can be the result of induced cell death among neuronal precursor cells. Model predictions indicate that neuron production is most greatly reduced when exposure occurs during the early part of neurogenesis, a time that corresponds to rapid rates of X cell replication (Figure 8). For the purposes of validating model predictions, there are few stereological studies estimating the total number of neurons in the neocortex following low-dose irradiation in the mouse. Schmidt and Lent (71) estimated that 40% reduction in neuron number, assessed at P60, following a 2 Gy exposure on E15, and a 53% reduction due to a 3Gy dose. Miki *et al*. (30) determined that

neuron production was reduced by 23.5% in the rat following a 1Gy exposure on E15, which would correspond to E14 in the mouse. Currently, our model cannot accurately predict neuron deficits following these large doses due to the lack of necrotic death and inflammation parameters.

Other studies have assessed reduced neuron production in specific regions of the brain following low doses *in utero*. Using a three-dimensional analysis to estimate neuron density, Schmitz *et al*. (72) determined that there was a 5% reduction in pyramidal neurons occupying layer V of the murine neocortex after a 50 cGy exposure on E13. Similar results were observed by Korr *et al.* (36). However, we would expect that the more superficial layers of the cortex (IV-III/II) would be more severely affected due to an exposure at this time. Accounting for all six layers, our model predicts a 35% reduction in neuron number due to this same exposure.

Additionally, a stereological estimate from Korr *et al.* (36) indicates a 16% reduction of neuron production in the adult (P180) murine hippocampus following a 50 cGy exposure on E13. The hippocampus develops at the same time as the neocortex and this observed reduction in the hippocampus may be a good indication of the effects in the neocortex. The lack of stereological estimates for the purpose of comparison is the primary limitation concerning the validity of the current model predictions.

With this limitation in mind, the model predicts significant reductions in neuron production following *in utero* radiation during neurogenesis. The effects within the neocortex are further exacerbated with alterations in the migratory behavior of newly formed neurons (73). When irradiation takes place during later neurogenesis, cell death has a minimal effect on neuron production and the alterations among the Y cell population are assumed to be due primarily to disrupted migration. For example, a 25 cGy dose on El5 leads to only a 1% reduction in neuron production. However, 6% of post-mitotic neurons are improperly located within the neocortex (N. DeFrank, unpublished data). Therefore, approximately 80% of the reduced neuron population is due to migration alterations and only 20% is accounted for by the induced cell death of X cells on E15.

In comparison, when exposure occurs early in neurogenesis (E11-E13), the loss of neurons due to cell death of neuronal precursor cells is extensive. For example, of the 40% decrease in size of the Y cell population on P5 following a 25 cGy exposure on E13, 85% is due to cell death and only 15% is due to slowed migration. This trend is expected because the early part of neurogenesis is marked by a greater size of the X cell population and faster replication rates. Overall, predictions indicate a steep dose-response relationship when low-dose irradiation occurs during the early days of neurogenesis and minimal effects when exposure takes place later in development (Figure 8).

DISCUSSION

The model provides a means for estimating the effects of low-dose radiation exposure on neuron production. To more accurately determine neuron loss in the neocortex following irradiation, parameters pertaining to necrotic cell death and alterations in phagocytic capacity

should be incorporated. With these additions, higher dose exposures could be assessed and clearance rates would be more accurate. Interestingly, the current model provides some indications as to the differences between high and low dose exposures. Specifically, Borovitskaya *et al*. (62) determined that the morphology of the nuclear remnants present 15 hours after the initial pyknosis no longer appear to be characteristic of apoptosis. This may reflect a secondary necrosis, which can occur when the growing numbers of apoptotic cells in a tissue diminish the probability for phagocytosis by neighboring cells. Our model estimates that cell clearance slows to 15 hours after a 40cGy exposure. Hence, the lack of cell clearance at high doses (~50 cGy) could be associated with the induced inflammation and subsequent serious malformations observed.

An underlying assumption in this cell death portion of the model is that there is only one wave of apoptosis immediately following exposure. This assumption is based on experimental data, in which the percentage of dead cells drops to normal levels within 24 hours of a low dose exposure (40) and within 48 hours of a high dose exposure (63). However, other studies have indicated that several waves of apoptosis occur due to an accumulation of reactive oxygen species (ROS). Radiation generates ROS, and following an exposure, sustained protein and lipid peroxidation may lead to later DNA damage and cell death. For example, Borges and Linden (74) determined that irradiation leads to two waves of apoptosis in certain cell populations within the rat retina. To account for this later cell loss, the kinetics of radiation-induced apoptosis needs to be further evaluated. The incorporation of later waves of apoptosis into the model will likely affect model predictions.

A second assumption of this cell death model is that post-mitotic cells are radio-resistant and Y cells maintain control rates of cell death. However, during the later period of neurodevelopment, neurons are sensitive to toxicants that may interfere with growth factor production or cell-cell communication. The process of physiological cell death following neurogenesis is regulated by growth factors and cytokines as well as by neurotransmitters (*2*). *In utero* radiation has been shown to cause alterations in synaptic connections and growth factor levels. Nakanishi *et al*. (75) demonstrated an increase in inhibitory synaptic connection in the rat neocortex following irradiation on E17. Other researchers have suggested that cortical neurons will die later in development following prenatal irradiation due to a lack of sufficient synaptic connections (76). Additionally, nerve growth factor (NGF) production in mouse neurons has been shown to be reduced following irradiation (77). Because radiation interferes with the processes regulating normal cell death, exposure may induce apoptosis in neurons that would not have otherwise been removed from the growing brain and our underlying assumption may not be valid. This experimental information will be incorporated into future model developments.

Recent radiation findings concerning the bystander effect have not been incorporated into the current model. The bystander effect is the adverse response of unexposed cells when neighboring cells are irradiated (78). Typically, this effect is more pronounced when the cells are grouped in high-density areas, where cell- cell contact and communication is high (79). Because we expected that cells on E11 would have the highest rates of cell death (in relationship to the high rates of replication), this bystander phenomenon might explain why we observe higher sensitivity of cells in the E13 mouse to undergo cell death in the VZ. At this

developmental time point, the VZ contains approximately 7 millions neuronal precursor cells, which is the peak density in this region across developmental time (Figure 8). In comparison, the proliferative region contains only 500,000 and 1 million cells on E11 and E15, respectively. Therefore, it is possible that E13 has the highest cell death rates due to the bystander effect. Future development of our radiation model will include potential bystander effects in an attempt to explain increased sensitivity during specific times.

There is a lack of comparable estimates of neuron production following *in utero* irradiation at low doses in rodent models, however comparison of the model output to behavioral endpoints can be informative. Table 3 displays the no observable adverse effect level (NOAEL) and the lowest observable adverse effect level (LOAEL) for behavioral effects in mice exposed to low doses of radiation during neurogenesis. Baskar & Uma Devi (*69*) determined that learning delays, assessed by the hole board test, were present in animals exposed to 35 cGy on E11.5 and E12.5. According to our model predictions, this corresponds to 10% of neuron improperly located within the neocortex on P5. Animals exposed on E14.5 did not demonstrate a learning delay until the exposure reached 50 cGy, related to a 5% reduction in neurons. Exposure on E17.5 did not affect learning behavior, and our model predicts very small decreases in neuron production after exposure at this time. A second study by Hossain & Uma Devi (*70*) determined the NOAEL for learning delays was 25 cGy when exposure occurred on E14. Model predictions indicate an 8% reduction in neurons.

The epidemiological evidence correlates with these animal data. Schull and Otake (*5*) found a significant decline in school performance rankings among those exposed *in utero* by the atomic bomb at 8-15 weeks, the time period of neurogenesis. No dose-response relationship was reported for these data. Additionally, IQ scores diminished linearly with increasing dose when exposure occurred between 8 and 15 gestational weeks. A significant decrease was also observed in children exposed between 16 and 25 weeks, but this effect was not as marked as compared to the exposure during the neurogenesis period. The estimated decrease in childhood IQ following irradiation during neurogenesis was 25 to 29 points per 100 cGy. Therefore, low doses of radiation exposures during susceptible times of gestation can lead to serious intellectual deficits. Our model indicates that radiation-induced cell loss is associated with the observed outcomes in humans and animals.

References

1. J. Berger-Sweeney and C. F. Hohmann. Behavioral consequences of abnormal cortical development: insights into developmental disabilities. *Behav Brain Re.* **86**, 121-42 (1997).
2. L.G. Costa, M. Aschner, A. Vitalone, T. Syversen, and O.P. Soldin**.** Developmental neuropathology of environmental agents. *Annu Rev Pharmacol Toxicol* **44,** 87-110 (2004).
3. P.M. Rodier. Environmental causes of central nervous system maldevelopment. *Pediatrics* **113,** 1076-83 (2004).
4. R.L. Brent. The effects of ionizing radiation, microwaves, and ultrasound on the developing

embryo: clinical interpretations and applications of the data. *Curr Probl Pediatr*. 14, 1-87 (1984).
5. W.J. Schull and M. Otake. Cognitive function and prenatal exposure to ionizing radiation. *Teratology* **59,** 222-6 (1999).
6. W.J. Schull. Ionising radiation and the developing human brain. *Ann ICRP* **22,** 95-118 (1991).
7. M. Otake and W.J. Schull. A review of forty-five years study of Hiroshima and Nagasaki atomic bomb survivors. Brain damage among the prenatally exposed. *J Radiat Res* **32**, 249-64 (1991).
8. B. Nad arajah, P. Alifragis, R.O. Wong, and J.G. Parnavelas. Neuronal migration in the developing cerebral cortex: observations based on real-time imaging. *Cereb Cortex* **13**, 607-11 (2003).
9. M.P. Ignacio, E.J. Kimm, G.H. Kageyama, J. Yu, and R.T. Robertson. Postnatal migration of neurons and formation of laminae in rat cerebral cortex. *Anat Embryol* **191**, 89-100 (1995).
10. J.F. Gadisseux, H.J. Kadhim, P. van den Bosch de Aguilar, V.S. Caviness, and P. Evrard. Neuron migration within the radial glial fiber system of the developing murine cerebrum: an electron microscopic autoradiographic analysis. *Brain Res Dev Brain Res* **52**, 39-56 (1990).
11. B.F. Uher and J. A. Golden. Neuronal migration defects of the cerebral cortex: a destination debacle. *Clin Genet* **58**, 16-24 (2000).
12. E.S. Anton, M.A. Marchionni, K.F. Lee, and P. Rakic. Role of GGF/neuregulin signaling in interactions between migrating neurons and radial glia in the developing cerebral cortex. *Development* **124**, 3501-10 (1997).
13. S. Fushiki, Y. Hyodo-Taguchi, C. Kinoshita, Y. Ishikawa, and T. Hirobe. Short- and long-term effects of low-dose prenatal X-irradiation in mouse cerebral cortex, with special reference to neuronal migration. *Acta Neuropathol* **93**, 443-9 (1997).
14. K. Hirai, H.Yoshioka, M. Kihara, K. Hasegawa, T. Sawada, and S. Fushiki. Effects of ethanol on neuronal migration and neural cell adhesion molecules in the embryonic rat cerebral cortex: a tissue culture study. *Brain Res Dev Brain Res* 118, 205-10 (1999).
15. J.E. Crandall, H.E. Hackett, S.A. Tobet, B.E. Kosofsky, and P.G. Bhide. Cocaine exposure decreases GABA neuron migration from the ganglionic eminence to the cerebral cortex in embryonic mice. *Cereb Cortex* **14**, 665-75 (2004).
16. N.H. Peckham and B. H. Choi. Abnormal neuronal distribution within the cerebral cortex after prenatal methylmercury intoxication. *Acta Neuropathol* **76**, 222-6 (1988).
17. S.H. Fatemi, E.S. Emamian, R.W. Sidwell, D.A. Kist, J.M. Stary, J.A. Earle, and P. Thuras. Human influenza viral infection in utero alters glial fibrillary acidic protein immunoreactivity in the developing brains of neonatal mice. *Mol Psychiatry* **7**, 633-40 (2002).
18. A. Hinoue, S. Fushiki, Y. Nishimura, K. Shiota. In utero exposure to brief hyperthermia interferes with the production and migration of neocortical neurons and induces apoptotic neuronal death in the fetal mouse brain." *Brain Res Dev Brain Res* **132**, 59-67 (2001).
19. C. Guerri. Neuroanatomical and neurophysiological mechanisms involved in central nervous system dysfunctions induced by prenatal alcohol exposure. *Alcohol Clin Exp Res* **22**, 304-12 (1998).
20. S.E. Arnold. Neurodevelopmental abnormalities in schizophrenia: insights from neuropathology. *Dev Psychopathol* **11**, 439-56 (1999).
21. Bentivoglio M, Tassi L, Pech E, Costa C, Fabene PF, Spreafico R. Cortical development and focal cortical dysplasia**.** *Epileptic Disord* **5**, S27-34 (2003).

22. B.S. Peterson. Neuroimaging in child and adolescent neuropsychiatric disorders. *J Am Acad Child Adolesc Psychiatry* **34**, 1560-76 (1995).
23. I. Ferrer, S. Alcantara, and E. Marti. A four-layered 'lissencephalic' cortex induced by prenatal X-irradiation in the rat. *Neuropathol Appl Neurobiol* **19**, 74-81 (1993).
24. I. Ferrer, S. Alcantara, M.J. Zujar, and C. Cinos. Structure and pathogenesis of cortical nodules induced by prenatal X-irradiation in the rat. *Acta Neuropathol* **85**, 205-12 (1993).
25. N. Chevassus-au-Louis and A. Represa. The right neuron at the wrong place: biology of heterotopic neurons in cortical neuronal migration disorders, with special reference to associated pathologies. *Cell Mol Life Sci* **15**, 1206-15 (1999).
26. I. Ferrer, S. Alcantara, M.J. Zujar, and C. Cinos. Structure and pathogenesis of cortical nodules induced by prenatal X-irradiation in the rat. *Acta Neuropathol (Berl).* **85**, 205-12 (1993).
27. C.J. D'Amato and S.P. Hicks. Effects of low levels of ionizing radiation on the developing cerebral cortex of the rat. *Neurology*. **15**, 1104-16 (1965).
28. M. Berry and J.T. Eayrs. The effects of x-irradiation on the development of the cerebral cortex. *J Anat*. 100, 707-22 (1966).
29. V.S. Caviness, T. Takahashi, and R.S. Nowakowski. Numbers, time and neocortical neuronogenesis: a general developmental and evolutionary model. *Trends Neurosci* **18**, 379-83 (1995).
30. T. Miki, Y. Fukui, Y. Takeuchi, and M. Itoh. A quantitative study of the effects of prenatal X-irradiation on the development of cerebral cortex in rats. *Neurosci Res* **23**, 241-7 (1995).
31. A. Kakita, K. Wakabayashi, M. Su, Y. Yoneoka, M. Sakamoto, F. Ikuta, and H. Takahashi. Intrauterine methylmercury intoxication. Consequence of the inherent brain lesions and cognitive dysfunction in maturity. Brain Res **22**, 322-30 (2000).
32. M.W. Miller. Kinetics of the migration of neurons to rat somatosensory cortex. *Brain Res Dev Brain Res* **115**, 111-22 (1999).
33. O. Ekshyyan and T. Y. Aw. Apoptosis in acute and chronic neurological disorders. *Front Biosci* **9**, 1567-76 (2004).
34. R.L. Margolis, D.M. Chuang, and R.M. Post. Programmed cell death: implications for neuropsychiatric disorders. *Biol Psychiatry* **35**, 946-56 (1994).
35. C.L. Limoli, E. Giedzinski, R. Rola, S. Otsuka, T.D. Palmer, and J.R. Fike. Radiation response of neural precursor cells: linking cellular sensitivity to cell cycle checkpoints, apoptosis and oxidative stress. *Radiat Res.* **161**, 17-27 (2004).
36. H. Korr, H. Thorsten Rohde, J. Benders, M. Dafotakis, N. Grolms, and C. Schmitz. Neuron loss during early adulthood following prenatal low-dose X-irradiation in the mouse brain. *Int J Radiat Biol* **77**, 567-80 (2001).
37. Y. Kameyama and M. Inouye. Irradiation injury to the developing nervous system: mechanisms of neuronal injury. *Neurotoxicology* **15,** 75-80 (1994).
38. G. Hildebrandt, M.P. Seed, C.N. Freemantle, C.A. Alam, P.R. Colville-Nash, and K.R. Trott. Mechanisms of the anti-inflammatory activity of low-dose radiation therapy. *Int J Radiat Biol* **74**, 367-78 (1998).
39. Ferrer, A. Macaya, R. Blanco, M. Olive, C. Cinos, F. Munell, and A.M. Planas. Evidence of internucleosomal DNA fragmentation and identification of dying cells in X-ray-induced cell death in the developing brain. *Int J Dev Neurosci* **13**, 21-8 (1995).
40. K. Hoshino and Y. Kameyama. Developmental-stage-dependent radiosensitivity of neural cells in the ventricular zone of telencephalon in mouse and rat fetuses. *Teratology* **37**, 257-

62 (1988).
41. Bolaris S, Bozas E, Benekou A, Philippidis H, Stylianopoulou F. In utero radiation-induced apoptosis and p53 gene expression in the developing rat brain. *Int J Radiat Biol* **77**, 71-81 (2001).
42. S. Norton and B. F. Kimler. Early effects of low doses of ionizing radiation on the fetal cerebral cortex in rats. *Radiat Res* **124**, 235-41 (1990).
43. B.F. Kimler. Prenatal irradiation: a major concern for the developing brain. *Int J Radiat Biol* **73**, 423-34 (1998).
44. E. Rola, J. Raber, A. Rizk, S. Otsuka, S.R. VandenBerg, D.R. Morhardt, and J.R. Fike. Radiation-induced impairment of hippocampal neurogenesis is associated with cognitive deficits in young mice. *Exp Neurol* **188**, 316-30 (2004).
45. B.G. Leroux, W.M. Leisenring, S.H. Moolgavkar, and E.M. Faustman. A biologically-based dose-response model for developmental toxicology. *Risk Anal* **16**, 449-58 (1996).
46. J.M. Gohlke, W.C. Griffith, S.M. Bartell, T.A. Lewandowski, and E.M. Faustman. A computational model for neocortical neuronogenesis predicts ethanol-induced neocortical neuron number deficits. *Dev Neurosci* **24**, 467-77 (2002).
47. T. Takahashi T, R.S. Nowakowski, and V.S. Caviness. The cell cycle of the pseudostratified ventricular epithelium of the embryonic murine cerebral wall. *J Neurosci* **15**, 6046-57 (1995).
48. T.F. Haydar, F. Wang, M.L. Schwartz, P. Rakic. Differential modulation of proliferation in the neocortical ventricular and subventricular zones. *J Neurosci* **20**, 5764-74 (2000).
49. K. Hoshino and Y. Kameyama. Developmental-stage-dependent radiosensitivity of neural cells in the ventricular zone of telencephalon in mouse and rat fetuses. *Teratology* **37**, 257-62 (1988).
50. D. Thomaidou, M.C. Mione, J.F. Cavanagh, J.G. Parnavelas. Apoptosis and its relation to the cell cycle in the developing cerebral cortex. *J Neurosci* **17**, 1075-85 (1997).
51. C. Verney, T. Takahashi, P. Bhide, R. Nowakowski and V. Caviness, Independent controls for neocortical neuron production and histogenetic cell death. *Developmental Neuroscience* **22**, 125–138 (2000).
52. J.M. Gohlke, W.C. Griffith, E.M. Faustman. The role of cell death during neocortical neurogenesis and synaptogenesis: implications from a computational model for the rat and mouse. *Brain Res Dev Brain Re*l **151**, 43-54 (2004).
53. T. Takahashi, R.S. Nowakowski, V.S. Caviness. The leaving or Q fraction of the murine cerebral proliferative epithelium: a general model of neocortical neuronogenesis. *J Neurosci* **19**, 6183-96 (1996).
54. M.W. Miller. Kinetics of the migration of neurons to rat somatosensory cortex. *Brain Res Dev Brain Res* **115**, 111-22 (1999).
55. N.C. Adams, T. Tomoda, M. Cooper, G. Dietz, and M.E. Hatten. Mice that lack astrotactin have slowed neuronal migration. *Development* **129**, 965-72 (2002).
56. J.C. Edmondson and M. E. Hatten. Glial-guided granule neuron migration in vitro: a high-resolution time-lapse video microscopic study. *J Neurosci* **7,** 1928-34 (1987).
57. E.S. Anton, M.A. Marchionni, K.F. Lee, P. Rakic. Role of GGF/neuregulin signaling in interactions between migrating neurons and radial glia in the developing cerebral cortex. *Development* **124**, 3501-10 (1997).
58. N.W. Seeds, M.F. Basham, S.P. Haffke. Neuronal migration is retarded in mice lacking the tissue plasminogen activator gene. *Proc Natl Acad Sci* **23**, 14118-23 (1999).

59. G. Leuba, D. Heumann, and T. Rabinowicz. Postnatal development of the mouse cerebral neocortex. I. Quantitative cytoarchitectonics of some motor and sensory areas. *J Hirnforsch* **18**, 461-81 (1977).
60. S. Fushiki, K. Matsushita, H. Yoshioka, and W.J. Schull. In utero exposure to low-doses of ionizing radiation decelerates neuronal migration in the developing rat brain. *Int J Radiat Biol* **70**, 53-60 (1996).
61. R. Licht, C.W. Jacobs, W.J. Tax, and J.H. Berden. An assay for the quantitative measurement of in vitro phagocytosis of early apoptotic thymocytes by murine resident peritoneal macrophages. J Immunol Methods 223, 237-48 (1999).
62. A.E. Borovitskaya, V.I. Evtushenko, and S.L. Sabol. Gamma-radiation-induced cell death in the fetal rat brain possesses molecular characteristics of apoptosis and is associated with specific messenger RNA elevations. Brain Res Mol Brain Res. 35, 19-30 (1996).
63. S. Nomoto, A. Ootsuyama, Y. Shioyama, M. Katsuki, S. Kondo, and T. Norimura. The high
64. susceptibility of heterozygous p53(+/-) mice to malformation after foetal irradiation is related to sub-competent apoptosis. Int J Radiat Biol 74, 419-29 (1998).
65. L. Bondolfi, M. Calhoun, F. Ermini, H.G. Kuhn, K.H. Wiederhold, L. Walker, M. Staufenbiel, and M. Jucker. Amyloid-associated neuron loss and gliogenesis in the neocortex of amyloid precursor protein transgenic mice. *J Neurosci* **22**, 515-22 (2002).
66. M.E. Calhoun, K.H. Wiederhold, D. Abramowski, A.L. Phinney, A. Probst, C. Sturchler-Pierrat, M. Staufenbiel, B. Sommer, and M. Jucker. Neuron loss in APP transgenic mice. *Nature* **395**, 755-6 (1998).
67. X.S. Sun, S. Takahashi, Y. Fukui, S. Hisano, Y. Kuboda, H. Sato, and M. Inouye. Different patterns of abnormal neuronal migration in the cerebral cortex of mice prenatally exposed to irradiation. *Brain Res Dev Brain Res* **114**, 99-108 (1999).
68. M. Inouye, S. Hayasaka, X.Z. Sun, and H. Yamamura. Disturbance of neuronal migration in mouse cerebral cortex by low-dose gamma-radiation. *J Radiat Res* **34**, 204-13 (1993).
69. S. Fushiki, Y. Hyodo-Taguchi, C. Kinoshita, Y. Ishikawa, T. Hirobe. Short- and long-term effects of low-dose prenatal X-irradiation in mouse cerebral cortex, with special reference to neuronal migration. *Acta Neuropathol* **93**, 443-9 (1997).
70. R. Baskar and P.U. Devi. Influence of gestational age to low-level gamma irradiation on postnatal behavior in mice. *Neurotoxicol Teratol* **22**, 593-602 (2000).
71. M. Hossain and P. Uma Devi. Effect of irradiation at the early foetal stage on adult brain function of mouse: learning and memory. *Int J Radiat Biol* **77**, 581-5 (2001).
72. S.L. Schmidt and R. Lent. Effects of prenatal irradiation on the development of cerebral cortex and corpus callosum of the mouse. *J Comp Neurol.* **264**, 193-204 (1987).
73. C. Schmitz, N. Grolms, P.R. Hof, R. Boehringer, J. Glaser, and H. Korr. Altered spatial arrangement of layer V pyramidal cells in the mouse brain following prenatal low-dose X-irradiation. A stereological study using a novel three-dimensional analysis method to estimate the nearest neighbor distance distributions of cells in thick sections. *Cereb Cortex*. **12**, 954-60 (2002).
74. S. Fushiki, Y. Hyodo-Taguchi, C. Kinoshita, Y. Ishikawa, and T. Hirobe. Short- and long-term effects of low-dose prenatal X-irradiation in mouse cerebral cortex, with special reference to neuronal migration. *Acta Neuropathol* **93**, 443-9 (1997).
75. H.L. Borges and R. Linden. Gamma irradiation leads to two waves of apoptosis in distinct cell populations of the retina of newborn rats. *J Cell Sci* **112**, 4315-24 (1999).

76. K. Nakanishi, K. Watanabe, M. Kawabata, A. Fukuda, and A. Oohira. Altered synaptic activities in cultures of neocortical neurons from prenatally X-irradiated rats. *Neurosci Lett*. **355**, 61-4 (2004).
77. Y. Abreu-Villaca, S.M. Schanuel, and S.L. Schmidt. Time course of the effects of prenatal gamma irradiation on the dorsal lateral geniculate nucleus of Swiss mice. *Int J Dev Neurosci*. **19**, 639-47 (2001).
78. Y. Dimberg and L. Larkfors. Effects of irradiation on cholinergic neurons and nerve growth factor mRNA in mouse foetal brain aggregation cultures. *Int J Radiat Biol*. **66**, 793-800 (1994).
79. Brooks AL. Evidence for 'bystander effects' in vivo. *Hum Exp Toxicol*. **23**, 67-70 (2004).
80. S.A. Mitchell, G. Randers-Pehrson, D.J. Brenner, and E.J. Hall. The bystander response in C3H 10T1/2 cells: the influence of cell-to-cell contact. *Radiat Res.* **161**, 397-401 (2004).

FIG. 1. Neuronal precursor cells (X cells) undergo three processes during neurogenesis: cell death (μ_1), replication (λ), and transformation (ν_1). X cells exiting the cell cycle become undifferentiated, migratory neurons (M cells) at a rate ν_1. M cells then transform into differentiated neurons (Y cells) once they cease migration at a biologically determined location. The rate at which cells transition from M cells to Y cells is represented by ν_2 and is dependent on the rate of movement along radial glial fibers (m) and the distance traversed during the migratory time period (d). Each cell population undergoes cell death at a rate μ.

FIG. 2. Rate parameters for computational modeling. A) The proportion of cells exiting the cell cycle (Q fraction) increases across the neurogenesis time period (E11 to E17 in the mouse). This fraction of cells was determined from the Takahashi et al. (53) dataset. Based on these data, the rate of cell cycle exit (ν_1) can be determined and is shown to increases across the eleven cell cycles. B) The distance migrating neurons are required to traverse increases across the developmental time frame. Data points during the embryonic period (days 11-18) are from Takahashi et al. (53) and the day 26 (P5) data point is from Leuba et al. (59). A loess regression line has been applied to these data. The rate at which M cells stop migrating and differentiate into Y cells is described by the rate ν_2. C) Dose-dependent alterations in the migration speed (m) of neurons along radial glia. These alterations are based on data generated by Fushiki et al. (60). Decreases in the migration rate are expressed as the fraction of the control speed. Polynomial and linear fits to the data points are presented.

FIG. 3. Model framework for Development (*21*). In this study, the model is applied to neocortex development. Type 'X' cells represent neuronal precursor cells in the proliferative regions. During each cell cycle, a precursor cell either stays in the proliferative region and undergoes further division (rate λ_1) or becomes a neuronal 'Y' cell (rate ν). Y cells are post-mitotic (rate $\lambda_2 = 0$). Both cell populations undergo cell death at unique rates (μ). Dead cells are removed from the population within some clearance time, ct.

FIG. 4. Rates of neuronal precursor cell replication (λ), death (μ), and differentiation (ν) occur at variable rates throughout neurogenesis in the fetal mouse. The early part of neurogenesis is marked by a rapid rate of replication among X cells. This rate corresponds to experimental data demonstrating the increasing length of the cell cycle during this time (42). Transformation rates are defined as the number of cells leaving the cell cycle (43). During the final day of neurogenesis, all remaining X cells differentiate (the transformation rate on E16-17 is 0.512/hr). Cell death among X cells is normally low in the developing neocortex (μ_1), however post-mitotic neurons (Y cells) undergo a period of extensive cell death (μ_2) during the postnatal period in the mouse.

FIG. 5. Predictions for neuronal precursors (X) and neurons (Y) in the control mouse brain. The number of X cells peak at E13.5, at which time the fraction of cells leaving the cell cycle and becoming Y cells increases. Without considering migration, the number of Y cells peak at E17. However, when the process of migration is included in the model, the transformation into Y cells is not complete until P5. Model predictions are compared to stereological estimates of neuron number in the adult mouse cerebral cortex adjusted for a 50% reduction in postnatal cell death due to normal cell death (·, 64; *, 65).

FIG. 6. Model predictions for the effects of radiation on neuronal migration in the neocortex. A) Radiation causes a decreased rate of transformation of migrating neuronal cells (M) into differentiated neurons (Y) by slowing the process of migration and leading to sustained numbers of M cells. In the mouse, migration is expected to end by P5. B) In irradiated animals, migration continues into later development, as observed by the slower increase in Y cells.

FIG. 7. Altered rates of neuronal precursor cell death following prenatal irradiation. A) Based on macrophage influx data (*19*), the ratio of macrophages to pyknotic cells can be calculated and related to an average clearance time across dose. B) The percentage of pyknotic cells in the murine neocortex following irradiation (*16*) was used in determining the increased cell death rates in the 24 hours following a low-dose exposure.

FIG. 8. Model predictions for the effects of radiation on cell death among neuronal precursors. The dose and time-dependent decrease of neuronal precursor cells following *in utero* irradiation leads to decreased neuron production.

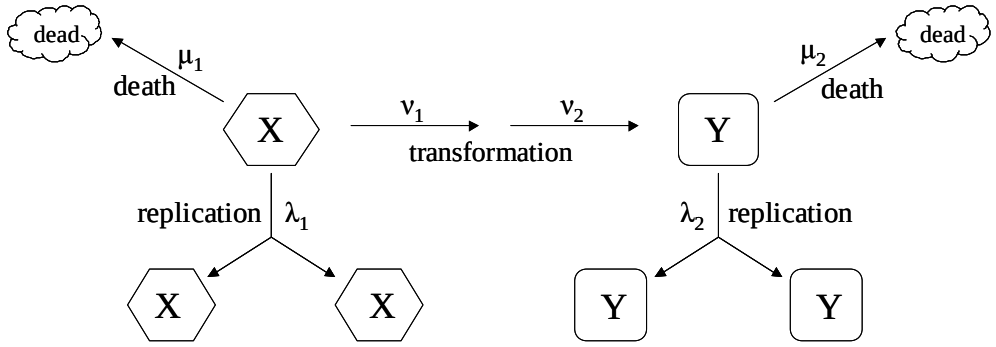
dead
μ1
death
X
ν1
transformation
ν2
Y
μ2
death
dead
replication
λ1
X
X
λ2
replication
Y
Y

FIG. 1.

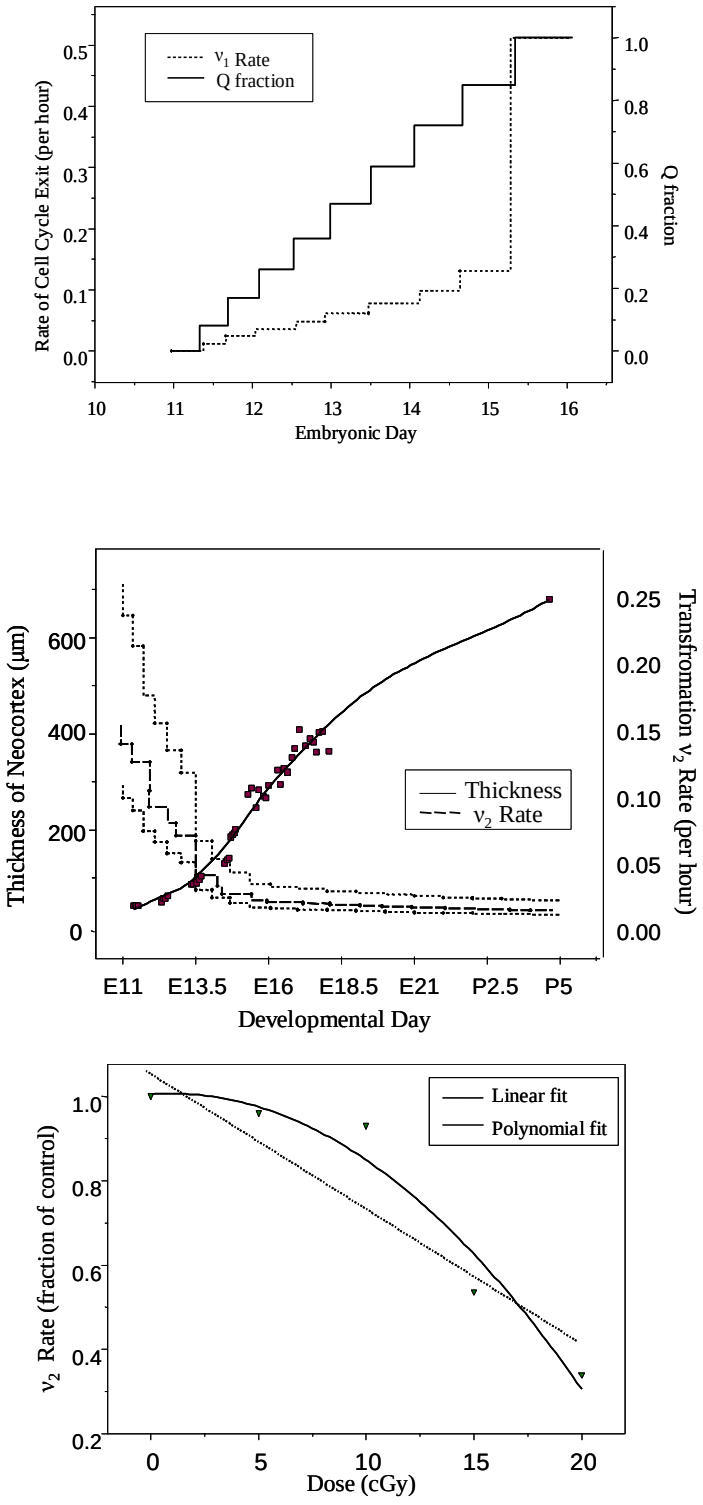
ν1 Rate
Q fraction
Rate of Cell Cycle Exit (per hour)
Q fraction
Embryonic Day
Thickness
ν2 Rate
Thickness of Neocortex (μm)
Transfromation ν2 Rate (per hour)
E11
E13.5
E16
E18.5
E21
P2.5
P5
Developmental Day
Linear fit
Polynomial fit
ν2 Rate (fraction of control)
Dose (cGy)

FIG. 2.

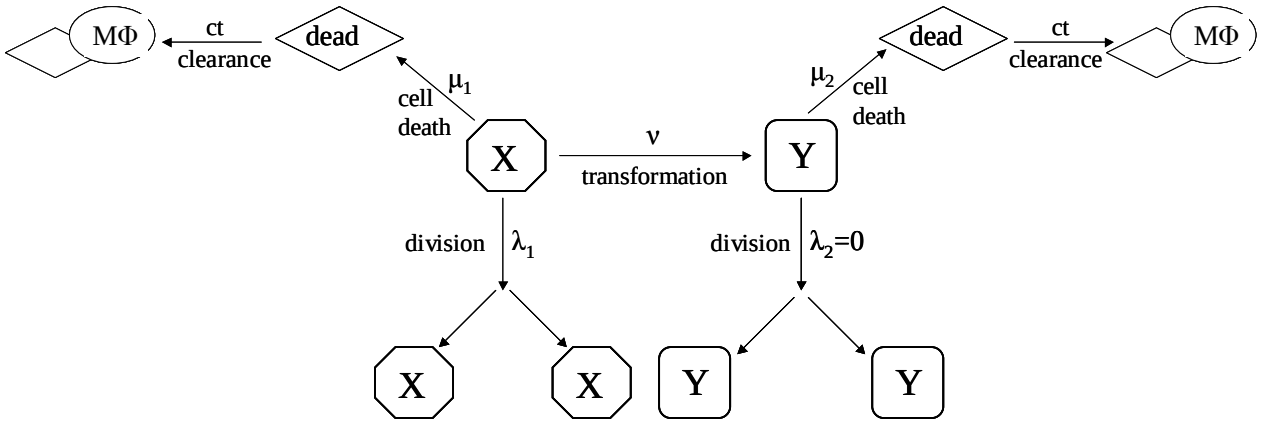
MΦ
ct
clearance
dead
μ1
cell
death
X
ν
transformation
Y
μ2
cell
death
dead
ct
clearance
MΦ
division
λ1
division
λ2=0
X
X
Y
Y

FIG. 3.

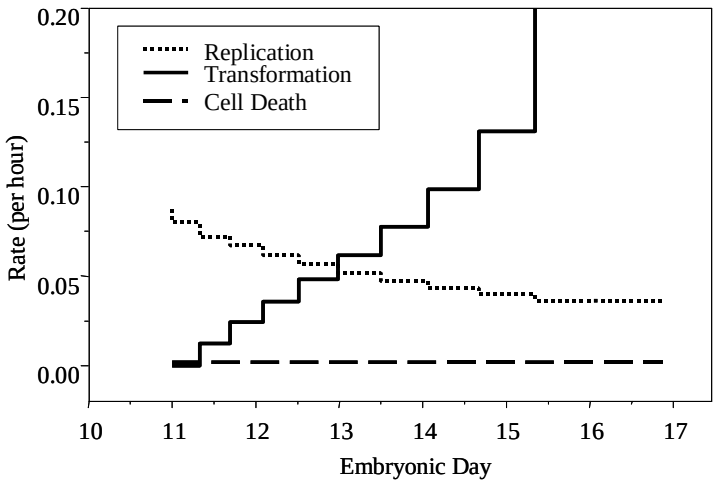
Replication
Transformation
Cell Death
Rate (per hour)
0.20
0.15
0.10
0.05
0.00
10
11
12
13
14
15
16
17
Embryonic Day

FIG. 4.

Fig 5

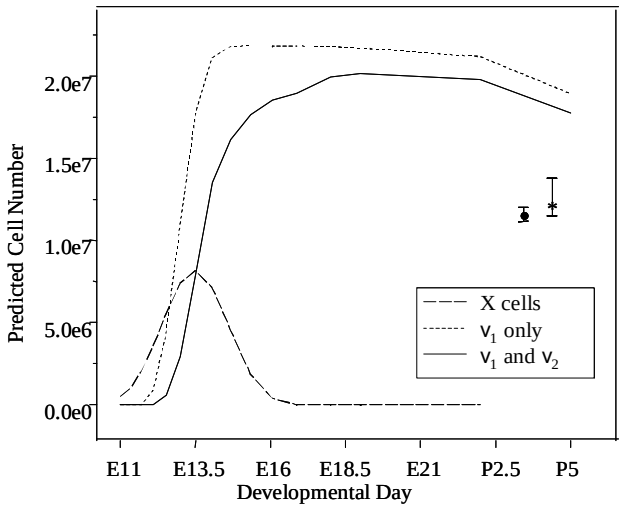
2.0e7
1.5e7
1.0e7
5.0e6
0.0e0
Predicted Cell Number
X cells
v1 only
v1 and v2
E11
E13.5
E16
E18.5
E21
P2.5
P5
Developmental Day

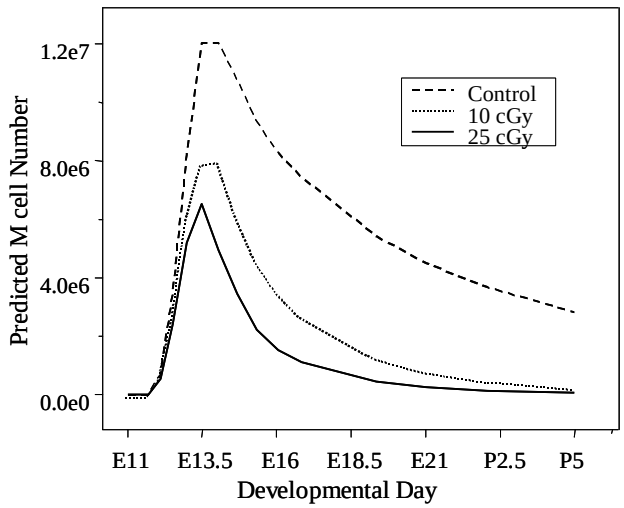
1.2e7
8.0e6
4.0e6
0.0e0
Predicted M cell Number
Control
10 cGy
25 cGy
E11
E13.5
E16
E18.5
E21
P2.5
P5
Developmental Day

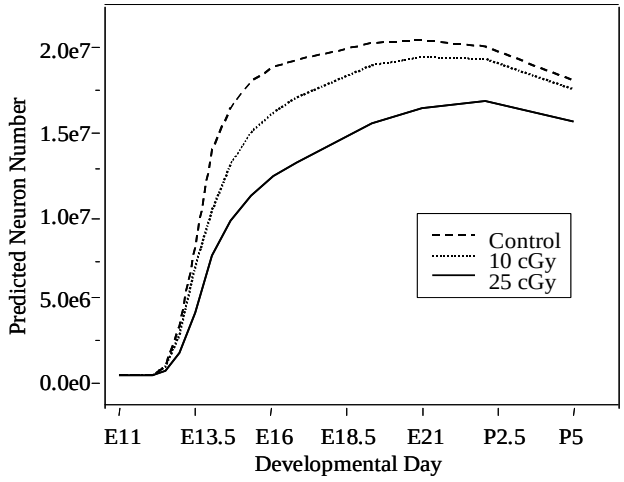
2.0e7
1.5e7
1.0e7
5.0e6
0.0e0
Predicted Neuron Number
Control
10 cGy
25 cGy
E11
E13.5
E16
E18.5
E21
P2.5
P5
Developmental Day

FIG. 6.

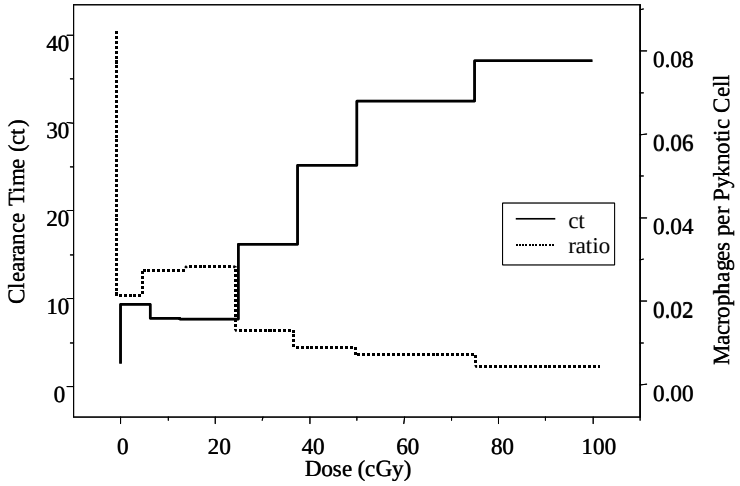
Clearance Time (ct)
Macrophages per Pyknotic Cell
Dose (cGy)
ct
ratio
0
10
20
30
40
0.00
0.02
0.04
0.06
0.08
0
20
40
60
80
100

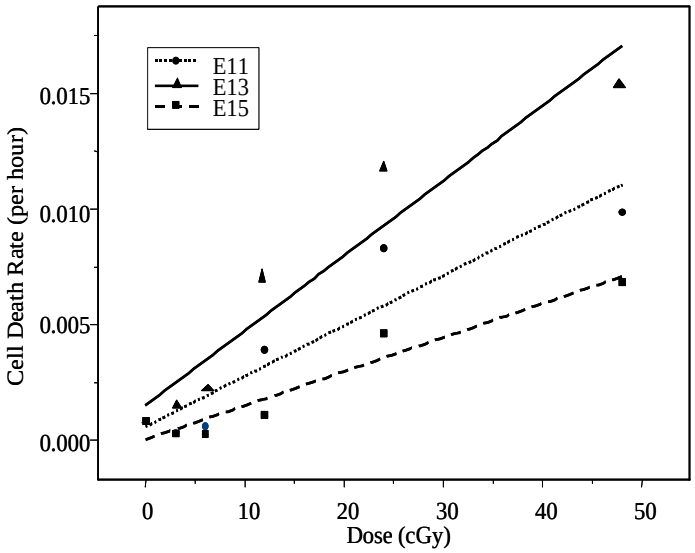
Cell Death Rate (per hour)
Dose (cGy)
E11
E13
E15
0.000
0.005
0.010
0.015
0
10
20
30
40
50

FIG. 7.

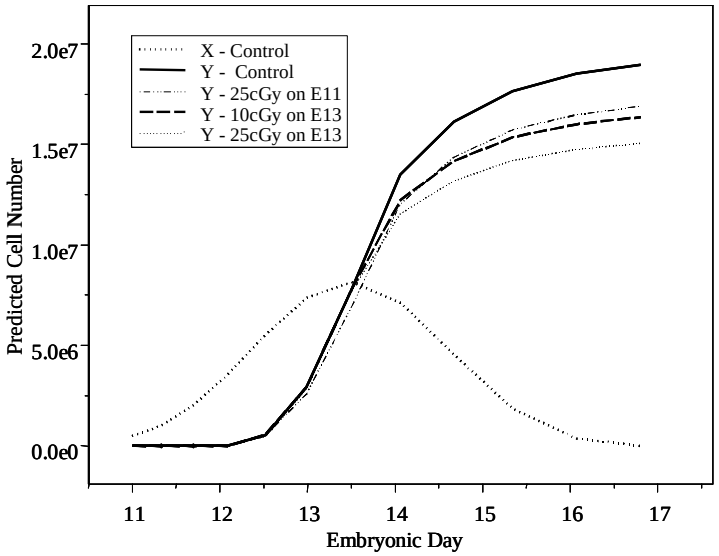
X - Control
Y - Control
Y - 25cGy on E11
Y - 10cGy on E13
Y - 25cGy on E13
Predicted Cell Number
2.0e7
1.5e7
1.0e7
5.0e6
0.0e0
11
12
13
14
15
16
17
Embryonic Day

FIG. 8.

TABLE 1

Summary of Neuronal Migration Studies

Reference	Species	System [a]	Methods	Rate μm/hr [b]
Takahashi et al. 1996	Mouse	in vivo, E14-17	^{3}H-dT and BUdR labeling	5.1
Miller 1999	Rat	in vivo, E15-21	^{3}H-dT labeling	5 (0.9)
Anton et al. 1997	Rat	cerebral cortex tissue, E18	cortical imprint assay	10.1 (0.3)
Edmondson 1987	Mouse	primary culture, P5-8	video microscopy	33 (20)
Adams et al. 2002	Mouse	purified neurons & glia, P6	video microscopy	12.5 (3)
Seeds et al. 1999	Mouse	cerebellar cortex tissue, P8	video microscopy	7.3 (0.8)

[a]The *in vitro* systems were used to assess how fast neurons travel along radial glial fibers only. *In vivo* estimates include radial glia dependent movement in addition to other forms of migration.

[b]Rates are expressed as μm per hour, with the standard deviation in parentheses when available.

TABLE 2

Neurogenesis Model Parameters

			Experimental Data Description		
Parameter	Exposure Status	Data	System	Time	Reference
Tc	Unexposed	Cell Cycle Length	Murine neocortex	E11-E17	*22*
Q	Unexposed	% Non-Cycling Cells	Murine neocortex	E11-E17	*23*
% Dead	Exposed	% Pyknotic Cells	Murine neocortex	E10, E13, E15	*15*
Xo	Unexposed	Founder Cell Population Count	Murine neocortex	E11	*24*
ct	Exposed	Macrophage Influx Phagocytic Capacity	Murine neocortex Murine thymocytes	E15 in vitro	*27*

TABLE 3

Behavior Studies[a] and Corresponding Model Predictions

Endpoint	LOAEL[b]	NOAEL[c]	Exposure	Reference	Y Cells[d] (% Control)
Locomotor activity	**25**	-	E14	Kimler & Norton 1988	95
	50	**35**	E11.5	Baskaret et al. 2000	89
Learning delay	50	**25**	E14	Hossain et al. 2001	95
	35	**25**	E11.5	Baskaret et al. 2000	90
Memory retention	50	**35**	E14.5	Baskaret al. 2000	94
	50	**25**	E14	Hossain et al. 2001	95
Exploratory activity	35	**25**	E12.5	Baskar et al. 2000	90

[a]Radiation-induced alterations in behavioral parameters across dose in young mice exposed to radiation *in utero* during neurogenesis.

[b]Lowest observable adverse effect level.

[c]No observable adverse effect level

[d]Model predictions, pertaining to improper migration following a NOEAL exposure on the treatment day, are included for comparison.